Annals of Operations Research
https://doi.org/10.1007/s10479-022-04760-x

ORIGINAL RESEARCH

A robust multi-objective model for healthcare resource management and location planning during pandemics

Levent Eriskin[1] · **Mumtaz Karatas**[1] · **Yu-Jun Zheng**[2]

Accepted: 29 April 2022

Abstract
In this study, we consider the problem of healthcare resource management and location planning problem during the early stages of a pandemic/epidemic under demand uncertainty. Our main ambition is to improve the preparedness level and response effectiveness of healthcare authorities in fighting pandemics/epidemics by implementing analytical techniques. Building on lessons from the Chinese experience in the COVID-19 outbreak, we first develop a deterministic multi-objective mixed integer linear program (MILP) which determines the location and size of new pandemic hospitals (strategic level planning), periodic regional health resource re-allocations (tactical level planning) and daily patient-hospital assignments (operational level planning). Taking the forecasted number of cases along a planning horizon as an input, the model minimizes the weighted sum of the number of rejected patients, total travel distance, and installation cost of hospitals subject to real-world constraints and organizational rules. Next, accounting for the uncertainty in the spread speed of the disease, we employ an across scenario robust (ASR) model and reformulate the robust counterpart of the deterministic MILP. The ASR attains relatively more realistic solutions by considering multiple scenarios simultaneously while ensuring a predefined threshold of relative regret for the individual scenarios. Finally, we demonstrate the performance of proposed models on the case of Wuhan, China. Taking the 51 days worth of confirmed COVID-19 case data as an input, we solve both deterministic and robust models and discuss the impact of all three level decisions to the quality and performance of healthcare services during the pandemic. Our case study results show that although it is a challenging task to make strategic level decisions based on uncertain forecasted data, an immediate action can considerably improve the response effectiveness of healthcare authorities. Another important observation is that, the

✉ Mumtaz Karatas
mkaratas@dho.edu.tr

Levent Eriskin
leriskin@dho.edu.tr

Yu-Jun Zheng
zyj@hznu.edu.cn

[1] Department of Industrial Engineering, National Defence University, Turkish Naval Academy, 34940 Tuzla, Istanbul, Turkey

[2] School of Information Science and Engineering, Hangzhou Normal University, Hangzhou 311121, Zhejiang, China

Published online: 21 May 2022

installation times of pandemic hospitals have significant impact on the system performance in fighting with the shortage of beds and facilities.

Keywords OR in health services · Location · Robust optimization · Healthcare resource management · Pandemic management

1 Introduction

Although most infectious diseases are preventable and/or treatable, the recent outbreak of the COVID-19 pandemic caused by a novel Coronavirus (SARS-CoV-2) showed that they continue to pose a significant danger to human health and mortality (Silal et al. 2020). Originated from Wuhan, Hubei province of China, the novel coronavirus was first reported to the World Health Organization (WHO) at the last day of 2019 by the Wuhan Municipal Health Commission. At the end of January 2020, WHO reported a total of 7818 confirmed cases in 19 countries and declared it as a pandemic on March 11th, 2020 (WHO 2020). At the time this paper was being written (January 22, 2021), the number of confirmed cases worldwide was declared as approximately 99 million with 2.2 million deaths (WHO 2021). The high spread speed and severe consequences on several aspects of community's lifestyle, including social, economic, environmental, political and other factors makes this pandemic unique.

During this global healthcare crisis, the health service related supply chains faced both supply shortages and demand growths which led to the propagation of disruptions. The extra demand which fluctuates with respect to the pace of the coronavirus spread in the population created a critical pressure on health systems. The burden caused by the pandemic-induced state of uncertainty as well as the fast spread speed of the virus have impacted the management and delivery of public health services, especially in resource-constrained settings (OECD 2020). For instance, in the Chinese experience, 6% of COVID-19 patients required ventilatory support after a critical care admission (Yang et al. 2020). However, the quickly increasing number of patients requiring mechanical ventilation led to the saturation of available resources such as intensive care unit (ICU) beds, other necessary equipment and trained healthcare personnel (Lee et al. 2020). Even in the early stages of the pandemic, only 25% of COVID-19 patients received intubation and ventilation. The situation further worsened towards the outbreak epicentre and the fatality rate showed a seven-fold increase presumably related to healthcare resource shortfall (Wu and McGoogan 2020; Ji et al. 2020). Similar bottlenecks in healthcare resources and their outcomes are also experienced in other hardest hit European countries such as Germany, Italy, United Kingdom, and Turkey. As a response to the tsunami of infected cases, the Chinese government implemented a centralized command and treatment system and strong measures to control sources of infection supported by community prevention (such as traditional medicine implementations) and control mechanisms (Zheng et al. 2020). At the epicentre of the outbreak, new infectious disease hospitals with larger capacities are built at strategic locations to accommodate more patients. These steps taken to fight with the shortage of beds and facilities needed to treat the outbreak are further supported by lower level decisions (e.g. converting general ward beds to ICU beds, and general hospitals to critical care hospitals) that are coordinated with local authorities and hospitals (Xie et al. 2020).

One of the main conclusions derived from studies which assess the hospital capacity management mechanisms during pandemics (e.g., Sarkar and Chakrabarti 2020; Moghadas et al.

2020; Verhagen et al. 2020) is that, if no action is taken to plan and expand the supply of healthcare resources, the rapid saturation of health systems is highly probable (Noronha et al. 2020). Hence, in order to achieve a certain preparedness level in fighting pandemics/epidemics, health authorities should consider implementing regional resource allocation and patient redistribution strategies as well as use of alternative healthcare facilities (Sun et al. 2014). As also stated in Toner and Waldhorn (2006), rather than adopting individual hospital response plans, such holistic and collaborative approaches both in planning and response phases would substantially improve the effectiveness of the overall response plan.

Building on lessons from the Chinese experience and response to the COVID-19 outbreak, in this paper we consider an early centralized planning and preparation of healthcare resources and facilities to ensure adequate health-system resource availability and capacity for continued care provision, particularly in the context of a pandemic or epidemic scenario. For this purpose, at the first step, we develop a multi-objective deterministic mixed integer linear program (MILP) to determine the best regional health resource and patient allocation plan among hospitals as well as the location and size decisions for newly built healthcare facilities. Our formulation seeks to minimize (1) the total number of patients that are rejected by hospitals due to capacity shortage, (2) the total travel distance of patients who are assigned to a hospital, and (3) the total installation cost of newly opened pandemic hospitals, subject to several real-world constraints and organizational rules.

Although resource management and location planning models developed for the private sector (e.g., sole proprietorships, partnerships, privately owned corporations) and the public sector (e.g., hospitals, police station, fire-fighting, civil defense) share similar objectives (e.g. maximize some kind of utility), they differ in the way that these objectives and constraints are formulated. In specific, private owners focus on economic concerns (i.e., system cost and profit), whereas non-monetary terms such as serving the society as a whole is the main concern for public DMs (Revelle et al. 1970). Since the problem we tackle is related to public service and its outcomes have potential impacts on the pandemic response management performance of governments, we prioritize the society benefit. In other words, we prefer the so-called *socially acceptable* or *socially preferable* course of action and adopt a robust optimization approach which accounts for the demand uncertainty during the pandemic. Hence, at the second stage, we propose a robust counterpart of the deterministic model which accounts for the whole spectrum of possible number of confirmed cases during a pandemic (including the worst-case) and still ensures a certain level of fairness among all patients. Then, we show the performance of our modelling approach using real-world data from Wuhan, China. The results obtained from the case study assist DMs and planners in better understanding the impact of decisions at various levels to the overall quality of healthcare services and related practices.

The remainder of this paper is organized as follows: Section 2 provides the related work on healthcare resource management and healthcare facility location planning and summarizes the key features and contributions of our study. Section 3 presents the assumptions and formal problem definition. Section 4 presents the deterministic model and its robust counterpart. Section 5 includes the numerical results for the case of Wuhan, China, an analysis of solution characteristics and discussion. Section 6 concludes the paper with a few remarks and possible future directions.

2 Related work

In this section, we review the literature related to our research topic. Since there exists a vast body of papers on healthcare resource management and facility location domain, we include a selection of the most relevant studies and categorize them into three groups as: (*i*) healthcare resource management studies, (*ii*) healthcare facility location studies during pandemics/epidemics, and (*iii*) studies which incorporate both healthcare resource management and facility location decisions.

2.1 Healthcare resource management studies

The concept of healthcare resource management includes activities related to the budgeting and allocation of resources (medical supplies, equipment, and personnel) which are critical to accomplish the goals of healthcare facilities. Brandeau (2005) presented a detailed review on the optimal resource allocation in epidemic settings. Today, healthcare industry generates large amounts of complex data about patients, disease diagnosis, hospitals resources, medical devices, etc. The existence of such data enables planners and researchers develop more efficient and effective decision making tools to manage these resources.

In our review of the literature, we encountered a number of studies which carry out observational work, e.g., cohort studies, cross-sectional studies, case-control studies, using real-world data, to assist decision-makers (DMs) in evaluating and enhancing the performance of healthcare facilities. As an example, considering the limited resources for trauma care along with other healthcare services, Mwandri et al. (2020) evaluated and identified possible improvement areas in trauma care management in Tanzanian hospitals. The authors carried out a cross-sectional study and suggested funding strategies for trauma-care services and pre-hospital services, adoption of standardized treatment protocols, and central regulation of clinical crew training. Among the observational studies which tackle healthcare resource management problems during the COVID-19 outbreak, Lee et al. (2020) considered the planning and management strategies of critical care resources at a single medical centre in Singapore in response to the COVID-19 outbreak. The authors proposed the redeployment of staff and conversion of general ward beds to ICU beds to address the manpower and patient capacity issues during the pandemic. They also made suggestions such as differential training programmes, mitigating staff ratios across ill patients, shifting nurses from other disciplines upon providing critical care training, diverting trained physiotherapists, dieticians, and pharmacists to ward duty. Similarly, Khichar et al. (2020) discussed the problem of pandemic preparedness for the COVID-19 outbreak from a single healthcare centre viewpoint. They focused on four preparedness criteria as: space management, personnel management, training, and infection prevention. They also highlighted that the success of a healthcare management plan is related to the strength and types of early actions undertaken to fight pandemics.

Administrators of hospitals make routine decisions related to the management of healthcare resources. Some examples include the planning of hospital supplies, number and schedule of staff, bed planning, etc. (Sharma and Mansotra 2014). Considering that the quality of these decisions are proportionate to the accuracy of the forecasts of the number of patients expected as well as their length of stay, some researchers proposed stochastic or robust modelling frameworks. Among them, Zinouri (2016) implemented a seasonal Autoregressive Integrated Moving Average (ARIMA) time series model to predict daily demand for surgical operations and proposed a scenario-based mixed integer linear program (MILP) to

generate nurse schedules with minimum monthly assignment cost. Bai and Zhang (2014), on the other hand, adopted a more holistic multi-hospital planning approach and considered the hospital capacity management during pandemics from patients' behavior perspective. They proposed a non-linear programming model which represents patients' behavior in hospital selection by incorporating travel time and service lead time. Their model aimed at balancing the health resources and patient loads among hospitals within a region. Considering a multi-hospital health resource redistribution problem during pandemics, Savachkin and Uribe (2012) developed a simulation optimization based decision support system which generates dynamic strategies for distributing limited health resources among hospitals. Their proposed model basically redistributes resources (e.g. vaccines and antivirals) remaining from previous allocations in response to changing demand. Similar to our study, the authors consider daily changes in the demand and solve the optimization problem at the beginning of every outbreak epoch (episode). Sun et al. (2014) optimized the allocation of healthcare resources and patients to an existing network of hospitals during an influenza outbreak. The authors adopted a medium-term planning horizon and proposed a MILP formulation which minimizes the total and maximum travel distance of patients. In their formulation they broke the entire planning horizon into shorter intervals and updated the disease transmission and other planning parameters.

In Oueida et al. (2018), the authors proposed a resource preservation net framework using Petri-net integrated with cloud and edge computing to improve the performance of daily operations and maintain a stable flow of patients with a focus on non-consumable healthcare resources (e.g. doctors, nurses, transporters, accountants, receptionists, physicians, technicians) in emergency departments. They also implemented a Discrete Event Simulation (DES) model to validate the feasibility of their proposed solution to reduce patient wait time and length of stay. In another similar study which considers staff absenteeism in healthcare units, Kang et al. (2019) developed a Mixed-Integer Non-Linear Programming (MINLP) based stochastic Petri-net model to minimize the queue of patients and required resources. They showed that planning resources with absenteeism improved the performance of healthcare systems in terms of operational utilization. In Kang et al. (2019) the authors proposed a MINLP model for planning resources in healthcare systems to improve patient's satisfaction. The formulation aimed to minimize patient queue and required amount of resources in a hospital while considering staff absenteeism.

As another important work that considers the resource allocation problem, Long et al. (2018) developed a two-stage model for determining when and where to assign treatment units during the outbreak's early phases of the 2014 West African Ebola outbreak. The first stage of their model forecasts the number of new cases using a dynamic transmission model. In the second stage, they implement a linear program (LP) and a deterministic finite-horizon dynamic programming algorithm which allocate resources over future time periods. Ordu et al. (2020) proposed a combined forecasting, optimisation and simulation model to determine the required number of beds and staff to meet the demand with the objective of maximizing the number of discharged patients. Similar to Oueida et al. (2018), they used a DES model to capture the uncertainty of the patient pathway within a hospital and an integer linear programming (ILP) model to determine optimal resource level in a single hospital. In a recent study, Du et al. (2020) considered an emerging Cholera outbreak and proposed a multi-period resource allocation problem. They formulated a nonlinear optimization model which incorporates a set of ordinary-differential-equations and updates disease transmission parameters over time on a rolling horizon basis. They account for the uncertainty in system dynamics parameters by implementing a scenario-based stochastic programming approach. The authors also demonstrated the effectiveness of their model on allocation policy suggestions under

antibiotic treatment and vaccination. Woodul et al. (2019) developed an integrated susceptible, infected, and recovered (SIR) model and surge capacity model to assess the healthcare performance of a region during a pandemic. In their model, they do not consider opening new health centers and adopt a capacitated shortest distance allocation model, i.e., infected people will attempt to access their second nearest hospital if the nearest hospital's capacity is reached. They show the performance of their model on a case study similar to the 1918 Spanish Flu pandemic.

2.2 Healthcare facility location planning studies

In addition to resource management problems at the tactical or operational level, the strategic planning of healthcare facility locations has attracted considerable attention from the OR&MS community as well as from practitioners and DMs in the medical and health sectors over several decades.

Similar to other location problems for public service facilities (e.g. police stations, fire stations, supply centers for humanitarian aid operations), incorrect healthcare facility location decisions have serious impacts on the community beyond cost and basic performance metrics. Among the recent review papers on healthcare facility location, Ahmadi-Javid et al. (2017) presented a comprehensive survey that classifies different types of non-emergency and emergency facilities in terms of location planning. Healthcare facilities that are hard to access are expected to be associated with increased morbidity and mortality (Ahmadi-Javid et al. 2017). The impact is further compounded when the planning of resources in facilities are carried out by conventional inefficient techniques.

Today there exists a vast literature on healthcare facility location models, which can be traced back as early as to 1970s (see Narula and Ogbu (1979) for an earlier review). For this reason, in this paper we limit our review of literature pertaining to healthcare facility location planning studies with the ones which consider location studies during pandemics/epidemics.

Among these studies, Buyuktahtakin et al. (2018) considered the 2014 West African Ebola and proposed a MIP formulation which determines the optimal amount, timing, and location of healthcare resources over a multi-period planning horizon. Their model aims to minimize the total number of infections and fatalities within a budget constraint. In a more recent study, Hashemkhani Zolfani et al. (2020) proposed an inter-criteria correlation (CRITIC) approach, a well-known Multi-Criteria Decision-Making (MCDM) tool, for selecting the location of a temporary hospital for COVID-19 patients. To show the applicability of the proposed methodology, they implemented the decision support framework in Istanbul, Turkey for selecting the best location among several candidate hospital locations. Ivanov (2020) developed a simulation-based approach to analyze and predict the impacts of epidemic outbreaks on the performance of the healthcare network supply chain. The author reports that the timing of the installing or closing healthcare facilities have significant impact on the system performance. Devi et al. (2021) formulated a MILP model for the problem of location-allocation of temporary testing laboratories during pandemics with the objective of cot and travel time minimization. In another study, Çakir et al. (2021) utilized a fuzzy MCDM procedure to determine the optimal locations for mobile pandemic test labs.

2.3 Combined location planning and resource management studies

There also exist a few studies which incorporate location decisions within the resource management planning framework. Among them, Anparasan and Lejeune (2019) developed

a deterministic Integer Linear Programming (ILP) epidemic response model which aims to determine the number, size, and location of healthcare facilities as well as allocation of medical staff and ambulances to patients for the 2010 cholera outbreak in Haiti. Their model maximizes the number of patients transferred from triage locations to hospitals. Carr and Roberts (2010), on the other hand, developed a simulation model integrated with a MILP optimization model for generating plans for responding large-scale disease outbreaks. In specific, the authors implemented a deterministic, compartmental population-based model to simulate the disease spread and call the MILP model when it is necessary to locate new hospitals. The MILP basically determines the locations of emergency response facilities and the allocation of patients to those hospitals as well as the number of staff necessary to maximize the number of patients served. Maleki Rastaghi et al. (2018) proposed a bi-objective MINLP formulation for a location and allocation problem with capacity planning decisions to design a healthcare facility network with a referral system. The formulation seeked to minimize the total network cost (costs associated with new facilities, services, and distance traveled by patients) and the maximum workload of opened facilities.

In another example, Pouraliakbarimamaghani et al. (2018) proposed a variant of the Maximal Covering Location Problem (MCLP) to locate hospitals, temporary emergency unit and warehouses, and allocate patients to hospitals during a mass casualty event. Their model incorporated three objectives as maximizing demand covered, minimizing distance between hospitals and centers and minimizing the distance between warehouses and temporary emergency units. They solve the model with the Non-dominated Sorting Genetic Algorithm (NSGA-II) and the Non-dominated Ranking Genetic Algorithm (NRGA).

Table 1 summarizes the basic characteristics of the aforementioned literature on healthcare resource management and location planning. The first two columns introduce the paper (year and authors). The third column categorizes the studies in terms of application domain, i.e. papers considering healthcare resource management problems and papers integrating location planning with healthcare resource management. The fourth column represents the underlying setting of the study, e.g., epidemics, pandemics, surgical operations, general services, etc. The fifth column states if the demand is certain (deterministic) or uncertain, and the sixth column displays the modelling approach implemented. Column seven summarizes the type of decisions that are considered in the study, i.e., location, patient allocation, resource allocation, sizing decisions. Column eight displays the scope of the study, i.e. studies considering a single hospital or multiple hospitals. Finally the ninth column lists the objectives of the studies.

The table reveals that, although several studies tackled the resource planning and/or hospital location planning problem under different objectives, scopes, and settings, a few of them considered uncertain demand and handled it explicitly by implementing a stochastic or robust optimization approach with a centralized decision-making perspective. The number of studies which consider all three level (strategic, tactical, and operational) decisions related to the location and sizing of hospitals as well as allocation of resources and patients to hospitals is limited. To the best of our knowledge, our study is the first one to consider uncertainty in a multiple scenario setting for a combined hospital site location and healthcare resource allocation problem.

2.4 Key features and contributions of the study

We summarize the main features and contributions of our work to the literature as follows:

(*i*) We approach the healthcare resource management problem from a holistic perspective and considering a centralized command and treatment system, we propose a formulation

Table 1 A synthesis of the healthcare resource management and location studies

Year	Author	Application domain(*)	Underlying setting	Demand	Modelling approach	Decision type				Scope	Objective
						Location	Patient allocation	Resource allocation	Sizing		
2010	Carr and Roberts	HRM & LoP	Epidemics	Uncertain	Simulation-based optimization (MILP formulation)	+	+	+	–	Multiple hospitals	Maximize the number of patients served
2012	Savachkin and Uribe	HRM	Influenza pandemics	Certain	Mathematical modelling (NLP formulation)	–	–	+	–	Multiple hospitals	Minimize expected societal and economic costs
2014	Bai and Zhang	HRM	Influenza pandemics	Certain	Mathematical modelling (NLP formulation)	–	+	–	–	Multiple hospitals	Minimize system cost
2014	Sun et al.	HRM	Pandemics	Certain	Mathematical modelling (MILP formulation)	–	+	+	–	Multiple hospitals	Minimize the total and maximum travel distance of patients
2016	Zinouri	HRM	Surgical operations	Uncertain	Mathematical modelling (Scenario-based MILP formulation)	–	–	+	–	Single hospital	Generate nurse schedules with minimum monthly assignment cost
2018	Maleki Rastaghi et al.	HRM & LoP	General services	Certain	Mathematical modelling (MINLP formulation)	+	+	+	–	Multiple hospitals	Minimize total network cost
											Minimize the maximum workload of opened facilities

Table 1 continued

Year	Author	Application domain(*)	Underlying setting	Demand	Modelling approach	Decision type				Scope	Objective
						Location	Patient allocation	Resource allocation	Sizing		
2018	Oueida et al.	HRM	Emergency Departments	Uncertain	Petri-net modelling and DES modelling	–	–	+	–	Single hospital	Minimize patient wait time and length of stay at the hospital
2018	Long et al.	HRM	Epidemics	Certain	– Mathematical modelling (LP formulation)	–	–	+	–	Multiple hospitals	Minimize new infections
					Finite-horizon dynamic programming						
2018	Pouraliakbari mamaghani et al.	HRM & LoP	Pandemics / Epidemics	Certain	Mathematical modelling (ILP formulation)	+	+	+	–	Multiple hospitals	Maximize demand covered
											Minimize distance between hospitals and centers
											Minimize distance between warehouses and temporary emergency units
2018	Buyuktahtakin et al.	HRM & LoP	Epidemics	Certain	Mathematical modelling (MILP formulation)	+	+	+	–	Multiple hospitals	Minimize the total number of infected individuals and deaths

Table 1 continued

Year	Author	Application domain(*)	Underlying setting	Demand	Modelling approach	Decision type				Scope	Objective
						Location	Patient allocation	Resource allocation	Sizing		
2019	Kang et al.	HRM	General services	Certain	Mathematical modelling (MILP formulation)	–	–	+	–	Single hospital	Minimize patient queue
											Minimize required amount of resources in a hospital
2019	Kang et al.	HRM	General services	Uncertain	MINLP-based stochastic Petri-net modelling	–	–	+	–	Single hospital	Minimize patient queue
											Minimize required resources
2019	Anparasan and Lejeune	HRM & LoP	Epidemics	Certain	Mathematical modelling (ILP formulation)	+	+	+	+	Multiple hospitals	Maximize the number of patients transported from triage locations to hospitals
2019	Woodul et al.	HRM	Pandemics	Certain	Integrated SIR and surge capacity model	–	+	–	–	Multiple hospitals	N/A
2020	Mwandri et al.	HRM	Injuries (trauma-care)	Certain	Observational	–	–	–	–	Three hospitals	Assessing in-hospital trauma-burden and major injury process of care

Table 1 continued

Year	Author	Application domain(*)	Underlying setting	Demand	Modelling approach	Decision type				Scope	Objective
						Location	Patient allocation	Resource allocation	Sizing		
2020	Lee et al.	HRM	Covid-19 pandemic	Certain	Observational	–	–	–	–	Single hospital	Improving resource utilisation
2020	Khichar et al.	HRM	Covid-19 pandemic	Certain	Observational	–	–	–	–	Single hospital	Assess the performance of preparedness measures
2020	Ordu et al.	HRM	General services	Uncertain	Simulation-based optimization (ILP formulation)	–	–	+	–	Single hospital	Maximize the number of discharged patients (throughput)
2020	Du et al.	HRM	Cholera epidemic	Uncertain	Integrated SIR and scenario-based stochastic optimization	–	–	+	–	Multiple hospitals	Determine the optimal strategy of intervention resource allocation
2020	Hashemkhani Zolfani et al.	HRM & LoP	Covid-19 pandemic	Certain	MCDM (CRITIC)	+	–	–	–	Single hospital	N/A
2021	Devi et al.	LoP	Covid-19 pandemic	Certain	Mathematical modelling (MILP formulation)	+	+	–	–	Multiple hospitals	Minimize total cost and travel time

Table 1 continued

Year	Author	Application domain(*)	Underlying setting	Demand	Modelling approach	Decision type				Scope	Objective
						Location	Patient allocation	Resource allocation	Sizing		
2021	Çakir et al.	LoP	Pandemics	Certain	MCDM	+	−	−	−	Multiple hospitals	Minimize contact with other patients
	This study	HRM & LoP	Covid-19 pandemic	Uncertain	Mathematical modelling (Robust MILP formulation)	+	+	+	+	Multiple hospitals	Minimize the total number of patients that are rejected by hospital
											Minimize the total travel distance of patients
											Minimize the total installation cost of newly opened pandemic hospitals

(*) HRM: Healthcare Resource Management; LoP: Location Planning

which incorporates strategic, tactical, and operational level decisions. In terms of strategic decisions, we determine the location and size of newly built pandemic hospitals. The decisions related to resource allocation among city hospitals and patient-hospital assignments are regarded as tactical and operational level decisions, respectively.

(*ii*) We propose a deterministic multi-objective MILP formulation which attempts to minimize the weighted sum of number of rejected patients, travel distance, and installation cost of pandemic hospitals. The MILP allows each decision type to be implemented at particular intervals (e.g., one time decision for strategic, bi-weekly for tactical, and daily for operational) in accordance with the governmental and/or organizational rules.

(*iii*) Considering that the weights assigned to each term of the objective function are inherently subjective and depend on the preference of the DM(s), we perform a a posteriori weight analysis where we solve the deterministic model for different weight combinations and carry out a sensitivity analysis with respect to individual and aggregated objective values.

(*iv*) The extent of spread speed and transmission as well as the severity of the disease may be unclear during the early stages of a pandemic. Thus, to account for the demand uncertainty and attain a more socially acceptable solution, we employ a robust optimization modelling approach. In particular, we employ an Across Scenario Robust (ASR) model which considers multiple scenarios simultaneously while obtaining solutions that keep the relative regret for each scenario under a predefined threshold.

(*v*) We demonstrate the performance of our proposed models on the case of Wuhan, China. Using 51 days worth of data (i.e., the number of confirmed COVID-19 cases) as an input, we solve both deterministic and robust models and discuss the impact of decisions at various levels to the quality of healthcare services during the pandemic. It should also be noted that, although we apply our model for the Chinese healthcare system, it can easily be modified with respect to the special needs and organizational rules of other countries.

3 Assumptions and problem framework

We consider a set of population centers $i \in I$ and a set of city hospitals $h \in H$. During the COVID-19 pandemic, several governments built temporary and/or permanent pandemic hospitals with different capacities to reduce the burden on city hospitals by providing additional hospital beds and other resources for patients. Hence, in our problem setting, we assume that there exist a set of discrete candidate locations denoted as $j \in J$ for building new pandemic hospitals of different sizes denoted as $s \in S$. Considering a resource-limited environment, we denote the set of resources as $r \in R$ and denote the available amount of resources of type r at each hospital h as Q_{hr}. For a newly established pandemic hospital of size $s \in S$, the amount of resource of type $r \in R$ is denoted as $\bar{Q}_{rs}$. ICU and non-ICU beds, support equipment (e.g., ventilators, computed tomography (CT) scan machines), and the critical care team (e.g., doctors, nurses, lab technicians) are some examples of patient management resources that stress healthcare facilities and systems during a pandemic, epidemic or other similar crises.

During the COVID-19 pandemic, most healthcare systems employed a rapid identification, diagnostic testing, and isolation of suspected cases in accordance with their triaging protocols. Based on their screening results and questionnaires, patients are stratified into COVID-19 risk levels and are admitted to non-ICU or ICU beds. For each patient type, there exist

different amounts of projected resources required to manage the illness during the pandemic surge. Hence, in our formulation, we categorize patients into different types depending on the outcome of their triage levels and define the set of patient types as $p \in P$. We then represent the specific amount of resources of type $r \in R$ required for each patient type p as β_{pr}. The burden on hospitals is further increased by the incoming regular patients, i.e., patients who seek medical service in non-COVID areas. Although these visits delay elective care to mitigate the spread of COVID-19 and create a significant pressure on healthcare systems, governments are responsible for carrying out public health services in non-pandemic areas. For this reason, at least a specific ratio of each resource type $r \in R$ (denoted by η_r) should be allocated to regular patients during the pandemic to maintain a certain level of other health services.

As a novel influenza virus emerges, the first set of decisions required by the national authorities involves whether to use a large-scale response and to devote alternative health resources and facilities to mitigate the impact (Lipsitch et al. 2009). Such responses may depend on the estimated risk posed by the outbreak in terms of spread speed, the expected number of cases, mortality rate, and other consequences. Being directly affected by those strategic-level decision, regional healthcare authorities face tactical level planning problems, e.g., determining an effective resource allocation plan among regional facilities as well as operational level problems, e.g., developing patient-hospital assignment and redistribution strategies. As also indicated previously, to enhance the overall performance of response actions to such outbreaks, regional pandemic planning must be linked to upper-level decisions. Consequently, in our modelling framework, we adopt a collaborative planning and decision-making approach at various levels to reflect on the nature and timing of decisions made during the initial weeks of the the pandemic/epidemic.

At this point, we consider three basic decision types as: *strategic*, *tactical*, and *operational*. Strategic decisions correspond to upper-level decisions related to opening new pandemic hospitals and their size (in terms of beds). During an outbreak, building new pandemic hospitals with relatively large ICU and non-ICU bed capacities plays an important role in meeting the growing demand and accommodating patients. Suppose that decisions are made for a planning horizon of length $|T|$ days and each day in the horizon is indexed as $t \in T$. We further assume that there exists a specific forecast for the number of cases expected at each day $t \in T$. In particular, we define d_{ipt} as the expected number of patients of type $p \in P$ at population center $i \in I$ observed at time period $t \in T$ and assume that these values are available to the DM at time $t = 0$. Taking the forecast as an input to our model, we would also like to note that generating forecasts is out of the scope of this study. We refer the interested reader to (Nikolopoulos et al. 2020; Ordu et al. 2020; Long et al. 2018) as they present excellent studies on the topic of forecasting during pandemics. In accordance with real-world implementations, new hospitals are assumed to be fully allocated to pandemic patients during the outbreak. These strategic decisions are represented via the binary variable y_{js} which takes a value of 1 is a pandemic hospital of size s is opened at location j and 0 otherwise.

Different from the strategic level decisions, we allow regional healthcare facilities (city hospitals) to implement tactical level decisions associated with the allocation of resources among healthcare facilities. These decisions are made regularly at the beginning of each period of length n days, denoted by $t \in D | D \subset T$. For this reason, we define the decision variable π_{hrt} which refers to the ratio of resources of type $r \in R$ at hospital $h \in H$ allocated to pandemic patients at decision time $t \in D$. We assume that resource allocation decisions remain unchanged between two consecutive decision time periods.

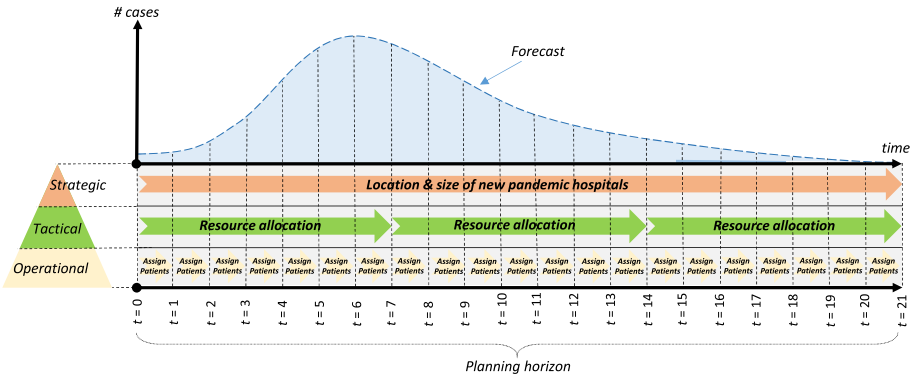

Fig. 1 Decision structure

Finally, at the lower-level, we incorporate operational decisions with the help of decision variables λ_{hipt} and $\bar{\lambda}_{jipt}$ which denote the ratio of patients of type $p \in P$ at location $i \in I$ allocated to a city hospital $h \in H$ at time period $t \in T$ and to a new pandemic hospital opened at location $j \in J$ at time period $t \in T$, respectively. These decisions are made daily by regional authorities and are closely related to the available capacity and resources of nearby hospitals for each population node i.

Figure 1 is a schematic of the main structure of our decision making process. Taking the forecasted number of patient types as an input to the proposed mathematical model, the figure shows an exemplary scheme for all three decision levels along a planning horizon of 21 days. The location and sizing (capacity) decisions for the new pandemic hospitals are made one time at the beginning of the planning horizon, i.e., at $t = 0$ and the decision stays in effect until the end of horizon. Tactical decisions pertaining the resource allocation decision among city hospitals are updated at the beginning of each 7 day long interval, whereas operational level decisions of patient allocations occur every day.

4 Formulations

Based on the aforementioned assumptions and the problem framework, we first formulate a deterministic MILP model for the problem, followed by its robust counterpart. We first would like to summarize the common notation before moving to the formulations.

Indices and sets

$i \in I$:	Set of population centers,
$j \in J$:	Set of candidate locations for new pandemic hospitals,
$h \in H$:	Set of city hospitals located in the region,
$p, p' \in P$:	Set of pandemic patient types,
$r \in R$:	Set of healthcare resource types,
$s \in S$:	Set of hospital size levels,
$g \in G$:	Set of objectives,
$t \in T$:	Set of time periods for operational-level decision making,
$D \subset T$:	Subset of time periods for tactical-level decision making,
$S_j \subset S$:	Subset of hospital size levels that can be installed at location $j \in J$.

Parameters

c_{js}: Cost of installing a pandemic hospital of size $s \in S$ to location $j \in J$,
d_{ipt}: Number of patients of type $p \in P$ at location $i \in I$ observed at time period $t \in T$,
$dist_{ij}$: Distance between locations $i \in I$ and $j \in J$,
$dist_{ih}$: Distance between locations $i \in I$ and $h \in H$,
$e_{pp'}$: Transition probability of a patient type p to type p' between two consecutive time periods,
e_{po}: Transition probability of a patient type p to outpatient between two consecutive time periods,
l_s: Days required to build a new pandemic hospital of size $s \in S$,
M: A relatively big number,
n: Number of days between two consecutive tactical-level decisions,
Q_{hr}: Amount of resource of type $r \in R$ at hospital $h \in H$,
$\bar{Q}_{rs}$: Amount of resource of type $r \in R$ at a newly installed pandemic hospital of size $s \in S$,
α_s: Minimum average number of patients that should be allocated to a new pandemic hospital of size $s \in S$,
β_{pr}: Amount of resource type $r \in R$ used by a patient of type $p \in P$,
η_r: Minimum ratio of resource type $r \in R$ that should be allocated to regular patients,
γ_{hp0}: Number of patients of type $p \in P$ at hospital $h \in H$ prior to the planning horizon (i.e. at time 0),
θ_g: Normalization factor for objective $g \in G$,
w_g: Weight of objective $g \in G$.

Decision variables

$$y_{js} = \begin{cases} 1, & \text{if a pandemic hospital of size } s \in S_j \text{ is opened at location } j \in J, \\ 0, & \text{otherwise,} \end{cases}$$

γ_{hpt} = Number of patients of type $p \in P$ at hospital $h \in H$ during time period $t \in T$,
$\bar{\gamma}_{jpt}$ = Number of patients of type $p \in P$ at hospital opened at $j \in J$ during time period $t \in T$,
λ_{hipt} = Ratio of patients of type $p \in P$ at pandemic location $i \in I$ allocated to hospital $h \in H$ at time period $t \in T$,
$\bar{\lambda}_{jipt}$ = Ratio of patients of type $p \in P$ at location $i \in I$ allocated to pandemic hospital opened at location $j \in J$ at time period $t \in T$,
π_{hrt} = Ratio of resources of type $r \in R$ at hospital $h \in H$ allocated to pandemic patients at decision time $t \in D$.

4.1 The deterministic model

Below is the formulation of the deterministic MILP model which we refer to as the model **(D)**.

Objective function
The model consists of three objectives each of which is aimed to be minimized. The first objective given by (1) aims to minimize the total number of patients that are rejected by hospitals due to capacity shortage. The second objective given by (2) aims to minimize the

total travel distance of patients that are assigned to a hospital. Finally, the third objective (3) aims to minimize the total installation cost of newly opened pandemic hospitals. We utilize the linear scalarizing approach to aggregate the objective functions, hence, the aggregated objective function is formulated as the weighted sum of these objectives as given in (4).

$$Obj\ 1 : \Phi_1 = \sum_{i\in I}\sum_{p\in P}\sum_{t\in T} d_{ipt}\left(1 - \sum_{h\in H}\lambda_{hipt} - \sum_{j\in J}\bar{\lambda}_{jipt}\right) \tag{1}$$

$$\begin{aligned} Obj\ 2 : \Phi_2 = &\sum_{h\in H}\sum_{i\in I}\sum_{p\in P}\sum_{t\in T} d_{ipt}\lambda_{hipt}dist_{ih} \\ &+ \sum_{j\in J}\sum_{i\in I}\sum_{p\in P}\sum_{t\in T} d_{ipt}\bar{\lambda}_{jipt}dist_{ij} \end{aligned} \tag{2}$$

$$Obj\ 3 : \Phi_3 = \sum_{j\in J}\sum_{s\in S_j} c_{js}y_{js} \tag{3}$$

$$\textbf{min} \sum_{g\in G} w_g\theta_g\Phi_g \tag{4}$$

In Eq. (4), the weighted objective terms are multiplied by the normalization factors θ_g. Utilized for removing the scaling effect caused by incommensurability of the objectives, normalization factors are computed as $\theta_g = 1 \Big/ \left(z_g^N - z_g^U\right)$ where z_g^N and z_g^U represent the Nadir and the Utopia points of each objective $g \in G$. Nadir and Utopia points essentially correspond to the maximum and minimum attainable values by these three objective terms, respectively.

Constraints

Demand satisfaction constraints: Constraint set (5) ensures that the total ratio of patients of type $p \in P$ allocated to all hospitals at time $t \in T$ from each demand node $i \in I$ is always less than or equal to 1. The first term of the equation represents the total ratio allocated to city hospitals and the second term refers to the ratio allocated to the newly established pandemic hospitals.

$$\sum_{h\in H}\lambda_{hipt} + \sum_{j\in J}\bar{\lambda}_{jipt} \le 1, \quad \forall i \in I, p \in P, t \in T \tag{5}$$

Constraints for computing the number of patients: Constraint sets (6)–(9) calculate the number of patients of each type $p \in P$ at each city hospital $h \in H$ and each newly installed pandemic hospital during time period $t \in T$. They simply consider the flow of incoming and outgoing patients and the number of patients remaining from the previous period.

$$\begin{aligned} \gamma_{hp1} = &\sum_{p'\in P}\gamma_{hp'0}e_{p'p} - \sum_{p'\in P\setminus\{p\}}\gamma_{hp0}e_{pp'} - \gamma_{hp0}e_{p0} \\ &+ \sum_{i\in I} d_{ip1}\lambda_{hip1}, \quad \forall h \in H, p \in P \end{aligned} \tag{6}$$

$$\begin{aligned} \gamma_{hpt} = &\sum_{p'\in P}\gamma_{hp'(t-1)}e_{p'p} - \sum_{p'\in P\setminus\{p\}}\gamma_{hp(t-1)}e_{pp'} - \gamma_{hp(t-1)}e_{p0} \\ &+ \sum_{i\in I} d_{ipt}\lambda_{hipt}, \forall h \in H, p \in P, t \in T \setminus \{1\} \end{aligned} \tag{7}$$

$$\bar{\gamma}_{jp1} = \sum_{i \in I} d_{ip1} \bar{\lambda}_{jip1}, \quad \forall j \in J, \forall p \in P \tag{8}$$

$$\bar{\gamma}_{hpt} = \sum_{p' \in P} \bar{\gamma}_{jp'(t-1)} e_{p'p} - \sum_{p' \in P \setminus \{p\}} \bar{\gamma}_{jp(t-1)} e_{pp'} - \bar{\gamma}_{jp(t-1)} e_{p0} + \sum_{i \in I} d_{ipt} \bar{\lambda}_{jipt}, \forall j \in J, p \in P, t \in T \setminus \{1\} \tag{9}$$

Resource constraints: Constraint set (10) ensures that the amount of resources used by the patients at city hospitals do not exceed the capacity allocated to pandemic patients. Similarly, constraint set (11) ensures that the total capacity of the newly installed hospitals are not exceeded.

$$\sum_{p \in P} \gamma_{hpt} \beta_{pr} \leq Q_{hr} \pi_{hrt'}, \quad \forall h \in H, r \in R, t' \in D, \{t \in T | t' \leq t \leq t' + n\} \tag{10}$$

$$\sum_{p \in P} \bar{\gamma}_{jpt} \beta_{pr} \leq \sum_{s \in S_j} \bar{Q}_{rs} y_{js}, \quad \forall j \in J, r \in R, t \in T \tag{11}$$

Services for regular patients: Constraint set (12) guarantees that the remaining ratio of each resource type at city hospitals is greater than the required level for regular patients.

$$\sum_{h \in H} Q_{hr} (1 - \pi_{hrt}) \geq \eta_r \sum_{h \in H} Q_{hr}, \quad \forall r \in R, t \in D \tag{12}$$

Hospital installation constraint: Constraint set (13) ensures that only a single facility can be installed at a suitable candidate location.

$$\sum_{s \in S_j} y_{js} \leq 1, \quad \forall j \in J \tag{13}$$

Time required to build a new hospital: Recall that it takes l_s days to build a new pandemic hospital of size $s \in S$. Therefore, the constraint set (14) ensures that no patient is assigned to a newly built hospital before its construction is finished.

$$\sum_{i \in I} \sum_{p \in P} \sum_{t | t \leq l_s} \bar{\lambda}_{jipt} \leq \left(1 - y_{js}\right) M, \quad \forall j \in J, s \in S_j \tag{14}$$

Condition to open a new hospital: Constraint set (15) guarantees that a new pandemic hospital can be opened only if the average number of patients allocated to the hospital of size $s \in S$ during the planning horizon is greater than the minimum level α_s. In other words, this constraint enforces an average utilization threshold for a new pandemic hospital to be installed.

$$\frac{1}{|T|} \sum_{p \in P} \sum_{t \in T} \bar{\gamma}_{jpt} \geq \sum_{s \in S_j} y_{js} \alpha_s, \quad \forall j \in J \tag{15}$$

Technical constraints: Constraint set (16) and (17) ensure that patients can be allocated to a newly opened pandemic hospital at location j only if a hospital is opened at that particular location and a hospital can be opened if patients are assigned to it.

$$M \sum_{s \in S_j} y_{js} \geq \sum_{i \in I} \sum_{p \in P} \sum_{t \in T} \bar{\lambda}_{jipt}, \quad \forall j \in J \tag{16}$$

$$\sum_{s \in S_j} y_{js} \leq M \sum_{i \in I} \sum_{p \in P} \sum_{t \in T} \bar{\lambda}_{jipt}, \quad \forall j \in J. \tag{17}$$

Variable domains:

$$y_{js} \in \{0,1\}, \quad \forall j \in J, s \in S_j \tag{18}$$
$$0 \leq \lambda_{hipt} \leq 1, \quad \forall h \in H, i \in I, p \in P, t \in T \tag{19}$$
$$0 \leq \bar{\lambda}_{jipt} \leq 1, \quad \forall j \in J, i \in I, p \in P, t \in T \tag{20}$$
$$0 \leq \pi_{hrt} \leq 1, \quad \forall h \in H, r \in R, t \in D \tag{21}$$
$$\gamma_{hpt} \geq 0, \quad \forall h \in H, p \in P, t \in T \tag{22}$$
$$\bar{\gamma}_{jpt} \geq 0, \quad \forall j \in J, p \in P, t \in T \tag{23}$$

4.2 The robust model

Health resource management and location planning for responding pandemics and/or epidemics inherently involve uncertainty due to lack of adequate information regarding problem parameters on the eve of the outbreak. Parameter uncertainty has been traditionally addressed with stochastic optimization models, examples of which can be seen widely in humanitarian logistics applications. These models specify closed-form probability distributions for unknown parameters that rely heavily on historical data. However, such reliable historical data are scarce and each pandemic/epidemic has *sui generis* properties that make it somewhat unique. Additionally, stochastic optimization models minimize the expected values of the objectives over all scenarios while neglecting individual scenarios (Paul and Wang 2019). This approach might lead to large relative regrets for some scenarios while health resource management and location planning decisions must perform consistently well across all scenarios. Conversely, robust optimization models focus on worst-case scenarios, which in return provide solutions that are overly conservative. From the risk perception perspective, stochastic optimization adapts a risk-neutral approach while robust optimization takes risk-averse attitude.

Considering the resource-limited environment faced during such crises, the implementation of solutions obtained for the worst-case scenarios may be demanding for most organizations in practice. The stochastic framework, on the other hand, has its own advantages in practice at the cost of probable unsatisfied demand. Hence, with all those aforementioned aspects of stochastic and robust optimization approaches in our minds, we prefer to utilize the p-robustness concept of Snyder and Daskin (2006) which essentially provides a compromise between the two modelling frameworks. Firstly, we define the additional sets, parameters, and decision variables, then we present the formulation and explain the details of the robust counterpart of the model **(D)** which we refer to as the across scenario robust **(ASR)** model.

Additional indices and sets

$\omega \in \Omega$: Set of scenarios.

Additional parameters

d_{ipt}^{ω}: Number of patients of type $p \in P$ at location $i \in I$ observed at time period $t \in T$ in scenario $\omega \in \Omega$,
ρ^{ω}: Probability of occurrence of each scenario $\omega \in \Omega$,
$\xi^{\omega *}$: Optimal objective function value of the model for scenario $\omega \in \Omega$,
τ: Relative regret threshold.

Additional decision variables

γ_{hpt}^{ω} = Number of patients of type $p \in P$ at hospital $h \in H$ during time period $t \in T$ in scenario $\omega \in \Omega$,

$\bar{\gamma}^{\omega}_{jpt}$ = Number of patients of type $p \in P$ at pandemic hospital opened at $j \in J$ during time period $t \in T$ in scenario $\omega \in \Omega$,
λ^{ω}_{hipt} = Ratio of patients of type $p \in P$ at location $i \in I$ allocated to hospital $h \in H$ at time period $t \in T$ in scenario $\omega \in \Omega$,
$\bar{\lambda}^{\omega}_{jipt}$ = Ratio of patients of type $p \in P$ at location $i \in I$ allocated to pandemic hospital opened at location $j \in J$ at time period $t \in T$ in scenario $\omega \in \Omega$,
π^{ω}_{hrt} = Ratio of resources of type $r \in R$ at hospital $h \in H$ allocated to pandemic patients at decision time $t \in D$ in scenario $\omega \in \Omega$,
ξ^{ω} = Objective function value of the model $(\mathbf{D}^{\omega})$ for a feasible solution indexed by $\omega \in \Omega$.

The model **(D)** essentially considers a single scenario (in other words, deterministic realizations of confirmed cases by period). Assuming that we have $|\Omega|$ possible scenarios, we may generate $|\Omega|$ distinct solutions that can be indexed with scenario ω. Being uncertain about the number of confirmed cases of districts on the eve of an outbreak of a pandemic, we would like to make sure that our a priori solution is satisfactory to some extent across the whole spectrum of scenarios. Accordingly, the p-robust model optimizes the expected value of the objective function across all scenarios while keeping the relative regret level of each scenario under a predefined threshold.

In the presence of multiple scenarios, the model **(D)** and its objective function value ξ are indexed by scenario $\omega \in \Omega$. Let $\xi^{\omega *}$ represent the optimal objective function value of the model $(\mathbf{D}^{\omega})$ for scenario ω. Let $\{y_{ij}, \gamma^{\omega}_{hpt}, \bar{\gamma}^{\omega}_{jpt}, \lambda^{\omega}_{hipt}, \bar{\lambda}^{\omega}_{jipt}, \pi^{\omega}_{hrt}\}$ be a feasible solution for all scenarios. Then this solution is referred to as p-robust for all scenarios such that;

$$\frac{\xi^{\omega} - \xi^{\omega *}}{\xi^{\omega *}} \leq \tau, \quad \forall \omega \in \Omega \tag{24}$$

where τ corresponds to the relative regret threshold (Snyder and Daskin 2006). For a particular fixed value of the relative regret threshold, the **(ASR)** model can be formulated as follows:

$$\min \sum_{\omega \in \Omega} \rho^{\omega} \xi^{\omega} \tag{25}$$

s.t.:

$$\xi^{\omega} \leq (1 + \tau)\xi^{\omega *}, \quad \forall \omega \in \Omega \tag{26}$$

$$\xi^{\omega} = \sum_{g \in G} w_g \theta^{\omega}_g \Phi^{\omega}_g, \quad \forall \omega \in \Omega \tag{27}$$

$$\sum_{h \in H} \lambda^{\omega}_{hipt} + \sum_{j \in J} \bar{\lambda}^{\omega}_{jipt} \leq 1, \quad \forall i \in I, p \in P, t \in T, \omega \in \Omega \tag{28}$$

$$\gamma^{\omega}_{hp1} = \sum_{p' \in P} \gamma_{hp'0} e_{p'p} - \sum_{p' \in P \setminus \{p\}} \gamma_{hp0} e_{pp'} - \gamma_{hp0} e_{p0} + \sum_{i \in I} d^{\omega}_{ip1} \lambda^{\omega}_{hip1}, \quad \forall h \in H, p \in P, \omega \in \Omega \tag{29}$$

$$\gamma^{\omega}_{hpt} = \sum_{p' \in P} \gamma^{\omega}_{hp'(t-1)} e_{p'p} - \sum_{p' \in P \setminus \{p\}} \gamma^{\omega}_{hp(t-1)} e_{pp'} - \gamma^{\omega}_{hp(t-1)} e_{p0} + \sum_{i \in I} d^{\omega}_{ipt} \lambda^{\omega}_{hipt}, \forall h \in H, p \in P, t \in T \setminus \{1\}, \omega \in \Omega \tag{30}$$

$$\bar{\gamma}^{\omega}_{jp1} = \sum_{i \in I} d^{\omega}_{ip1} \bar{\lambda}^{\omega}_{jip1}, \quad \forall j \in J, p \in P, \omega \in \Omega \tag{31}$$

$$\bar{\gamma}^{\omega}_{hpt} = \sum_{p' \in P} \bar{\gamma}^{\omega}_{jp'(t-1)} e_{p'p} - \sum_{p' \in P \setminus \{p\}} \bar{\gamma}^{\omega}_{jp(t-1)} e_{pp'} - \bar{\gamma}^{\omega}_{jp(t-1)} e_{p0}$$
$$+ \sum_{i \in I} d^{\omega}_{ipt} \bar{\lambda}^{\omega}_{jipt}, \forall j \in J, p \in P, t \in T \setminus \{1\}, \omega \in \Omega \quad (32)$$

$$\sum_{p \in P} \gamma^{\omega}_{hpt} \beta_{pr} \leq Q_{hr} \pi^{\omega}_{hrt'}, \quad \forall h \in H, r \in R, t' \in D,$$
$$\{t \in T | t' \leq t \leq t' + n\}, \omega \in \Omega \quad (33)$$

$$\sum_{p \in P} \bar{\gamma}^{\omega}_{jpt} \beta_{pr} \leq \sum_{s \in S_j} \bar{Q}_{rs} y_{js}, \quad \forall j \in J, r \in R, t \in T, \omega \in \Omega \quad (34)$$

$$\sum_{h \in H} Q_{hr} (1 - \pi^{\omega}_{hrt}) \geq \eta_r \sum_{h \in H} Q_{hr}, \quad \forall r \in R, t \in D, \omega \in \Omega \quad (35)$$

$$\sum_{s \in S_j} y_{js} \leq 1, \quad \forall j \in J \quad (36)$$

$$\sum_{i \in I} \sum_{p \in P} \sum_{t | t \leq l_s} \bar{\lambda}^{\omega}_{jipt} \leq \left(1 - y_{js}\right) M, \quad \forall j \in J, s \in S_j, \omega \in \Omega \quad (37)$$

$$\frac{1}{|T|} \sum_{p \in P} \sum_{t \in T} \bar{\gamma}^{\omega}_{jpt} \geq \sum_{s \in S_j} y_{js} \alpha_s, \quad \forall j \in J, \omega \in \Omega \quad (38)$$

$$M \sum_{s \in S_j} y_{js} \geq \sum_{i \in I} \sum_{p \in P} \sum_{t \in T} \bar{\lambda}^{\omega}_{jipt}, \quad \forall j \in J, \omega \in \Omega \quad (39)$$

$$\sum_{s \in S_j} y_{js} \leq M \sum_{i \in I} \sum_{p \in P} \sum_{t \in T} \bar{\lambda}^{\omega}_{jipt}, \quad \forall j \in J, \omega \in \Omega \quad (40)$$

$$y_{js} \in \{0, 1\}, \quad \forall j \in J, s \in S_j \quad (41)$$

$$0 \leq \lambda^{\omega}_{hipt} \leq 1, \quad \forall h \in H, i \in I, p \in P, t \in T, \omega \in \Omega \quad (42)$$

$$0 \leq \bar{\lambda}^{\omega}_{jipt} \leq 1, \quad \forall j \in J, i \in I, p \in P, t \in T, \omega \in \Omega \quad (43)$$

$$0 \leq \pi^{\omega}_{hrt} \leq 1, \quad \forall h \in H, r \in R, t \in D, \omega \in \Omega \quad (44)$$

$$\gamma^{\omega}_{hpt} \geq 0, \quad \forall h \in H, p \in P, t \in T, \omega \in \Omega \quad (45)$$

$$\bar{\gamma}^{\omega}_{jpt} \geq 0, \quad \forall j \in J, p \in P, t \in T, \omega \in \Omega \quad (46)$$

$$\xi^{\omega} \geq 0, \quad \forall \omega \in \Omega \quad (47)$$

Fundamentally, increasing the relative regret threshold (τ) relaxes the model **(ASR)** while decreasing the threshold tightens it. Hence, the choice of relative regret threshold affects the feasibility of a solution. Small regret for each scenario is desirable, therefore, a solution that has as small relative regret threshold as possible is seeked. In order to find a bound on τ, we utilized a practical two-step approach (Paul and Wang 2019). Not guaranteeing to generate the tightest possible bound τ, this computationally efficient procedure provides reasonable bounds. Steps of this procedure are given in Fig. 2.

Step 1.1 of the procedure optimizes $|\Omega|$ separate deterministic models. Step 1.2 obtains a stochastic optimization solution that minimizes the expected objective function value across all scenarios. Based on this solution, the relative regret for each scenario is computed and the upper bound for the relative regret threshold is set to the maximum relative regret value. In Step 2 of the procedure, the model **(ASR)** is tightened by decreasing τ^{UB} gradually until the

Step 1. **Initialization**

1.1 Optimize the model $(\mathbf{D}^{\omega})$ to obtain optimal $\xi^{\omega *}$ for each scenario ω.

1.2 Optimize the model **(ASR)** ignoring constraints (26) to obtain solution $\{y_{ij}, \gamma^{\omega}_{hpt}, \bar{\gamma}^{\omega}_{jpt}, \lambda^{\omega}_{hipt}, \bar{\lambda}^{\omega}_{jipt}, \pi^{\omega}_{hrt}\}$ and ξ^{ω} for each scenario ω.

1.3 Calculate the relative regret τ^{ω} for each scenario ω where $\tau^{\omega} = \frac{\xi^{\omega} - \xi^{\omega *}}{\xi^{\omega *}}$.

1.4 Set $\tau^{UB} = \max(\tau^{\omega})$ and $t = 1$. Go to Step 2.

Step 2: **Solve model (ASR) recursively by decreasing τ^{UB} until infeasibility occurs**

2.1 Optimize the model **(ASR)** by setting $\tau = \tau^{UB}(\zeta)$ where ζ is the scaling factor. Stop if infeasibility occurs. If the solution is feasible, obtain $\{y_{ij}, \gamma^{\omega}_{hp}, \bar{\gamma}^{\omega}_{jp}, \lambda^{\omega}_{hip}, \bar{\lambda}^{\omega}_{jip}, \pi^{\omega}_{hr}\}_t$, and let ξ^{ω}_t be the objective function value of scenario ω at iteration t.

2.2 Calculate incumbent relative regret as $\tau^{\omega}_t = \frac{\xi^{\omega}_t - \xi^{\omega *}}{\xi^{\omega *}}$. Set $\tau^{UB} = \max_{\omega}(\tau^{\omega}_t)$ and $t = t + 1$. Go to Step 2.1.

Fig. 2 Pseudo-code of the procedure

model becomes infeasible. The choice of scaling factor ζ is a subjective decision, however, can be tuned to obtain more precise upper bounds.

5 Case of Wuhan

We now apply the proposed models to the case of Wuhan where the novel coronavirus was first reported to the WHO at the last day of 2019. We take the starting day of the planning horizon as January 27th, 2020, the time when strategic, operational and tactical decisions are made by the authorities. The planning horizon consists of 51 days for which daily data of confirmed cases are available. After March 17th, 2020 the number of confirmed cases diminishes to zero, which marks the end of the planning horizon. In this numerical study, we treat the empirical daily confirmed case data of Wuhan as the forecasted data at the beginning of a pandemic. We first provide information regarding the data, then present and discuss the solutions of the models **(D)** and **(ASR)**.

5.1 Background and case study data

There are 14 administrative regions in Wuhan that are considered as the demand centers. All confirmed COVID-19 cases have been reported based on these regions. The breakdown of the number of confirmed cases with respect to regions and the severity levels (ICU, non-ICU) of the cases are shown in Fig. 3. Before the outbreak of the pandemic, there were 36 city hospitals with different capabilities in Wuhan that provide various types of healthcare to the habitants. All these hospitals have different resources available in terms of ICU bed, non-ICU bed, ventilator, computed tomography, Extracorporeal Membrane Oxygenation (ECMO), doctor, nurse and lab technician. Among 36 city hospitals, six of them do not provide ICU care. Even though the healthcare personnel have different professions, they can be allocated to pandemic treatment services based on emerging requirements.

After the outbreak of the pandemic, the administration determined 32 candidate locations for installing new pandemic hospitals. There are three different pandemic hospital sizes, namely, small, medium, and large, that can be installed on these locations based on the acreages. Among the 32 candidate locations, four of them are eligible for installing small size hospitals while 20 of them for medium and eight of them for large size hospitals. Note

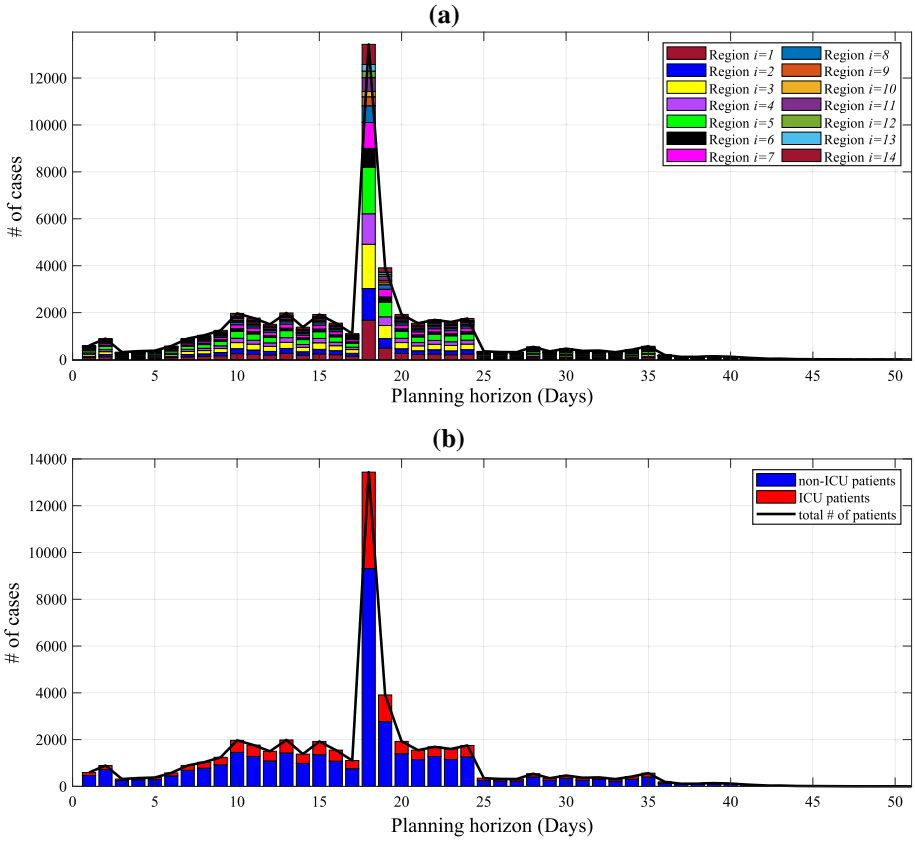

Fig. 3 The breakdown of the number of patients with respect to **(a)** 14 administrative regions (each color represents a specific region), and **(b)** ICU and non-ICU types. (Color figure online)

that a medium (large) size implies that a small (small and medium) size hospital can also be installed at that location. As expected, hospitals with different sizes have also different capabilities based on the amount of resources that can be allocated. Locations for the 14 administrative regions, 36 city hospitals, and 32 candidate sites for building new pandemic hospitals are illustrated in Fig. 4. The standard amount of resources that are allocated to hospitals with each size are summarized in Table 2.

The time required to install a new pandemic hospital varies according to hospital size. In the course of the COVID-19 crisis, the Huoshenshan Hospital with a capacity of 1000 beds was built in nine days between January 23rd, 2020 and February 2nd, 2020 near the Zhiyin Lake in the Caidian District, Wuhan. The hospital became fully operational on February 3rd, 2020, only 10 days after the construction began (Luo et al. 2020). Similarly, the construction of another emergency specialty field hospital in response to the COVID-19 pandemic, the Leishenshan Hospital was completed in only 12 days. Located at No.3 Parking Lot of the Athletes Village in Jiangxia District, Wuhan, Hubei, this hospital had a capacity of 1600 beds (Luo et al. 2020). As an earlier example, located in Beijing, Xiaotangshan SARS Hospital was buit in six days with a capacity of 1000 beds and began operating on the seventh day in response to the SARS epidemic in 2003 (Yang and Cheng 2020). Considering these examples,

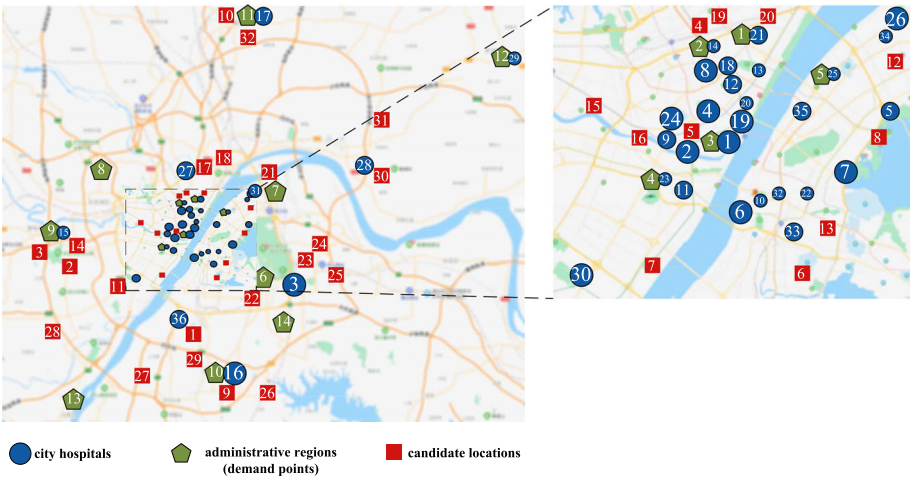

Fig. 4 Administrative regions, city hospitals, and candidate locations for new pandemic hospitals in Wuhan

Table 2 Amount of resources to be allocated to different size pandemic hospitals

r	Resource type	Hospital size		
		Small ($s = 1$)	Medium ($s = 2$)	Large ($s = 3$)
1	ICU Bed	100	400	600
2	Non-ICU Bed	200	800	1200
3	Ventilator	120	480	720
4	Tomography	5	20	30
5	ECMO	2	7	10
6	Doctor	58	233	350
7	Nurse	130	517	775
8	Lab Technician	24	95	143

Table 3 Resources consumed by patients based on severity level

p	Patient type	Resource type							
		ICU Bed	Non-ICU Bed	Ventilator	Tomography	ECMO	Doctor	Nurse	Lab Technician
1	ICU	1	–	0.8900	0.0417	0.0083	0.2500	0.6250	0.1430
2	Non-ICU	–	1	0.0500	0.0139	0	0.1670	0.3300	0.0476

we take the installation times of small (300 beds), medium (1200 beds), and large (1800 beds) size pandemic hospitals as 4, 11, and 13 days, respectively. Installation cost of each candidate pandemic hospital is estimated based on the location and size of the hospital. Based on the estimated figures, the average installation costs of pandemic hospitals are 22,843, 68,678, and 93,000 ¥ for small, medium, and large size hospitals, respectively.

Each hospitalized patient consumes the hospital resources required for the treatment according to the severity level. Based on empirical data and experience, the estimated amounts of daily resources consumed by each type of patient are given in Table 3.

Table 4 Transition probabilities of patients with different severity levels

Severity level (day t)	Severity level (day $t+1$)			
	Non-ICU	ICU	Cured	Death
ICU	0.03760	0.90388	0.05560	0.00292
Non-ICU	0.87481	0.04590	0.07840	0.00089

Table 5 Ratio of resources of city hospitals that should be allocated to regular patients

	Resource type							
	ICU Bed	Non-ICU Bed	Ventilator	Tomography	ECMO	Doctor	Nurse	Lab Technician
Allocated ratio	18%	15%	18%	30%	15%	18%	18%	40%

Table 4 provides the transition matrix that represents the daily transition probabilities of patients with different severity levels to the other patient types. These figures are estimated based on empirical data for the COVID-19 cases in Wuhan. To illustrate, a non-ICU patient becomes an ICU patient the next day with a probability of 0.0459, while his/her severity status remains the same with a probability of 0.87481. Cured and death statuses essentially correspond to the situation where the patient is discharged from the hospital.

Newly installed pandemic hospitals are intended to serve to pandemic patients only. On the other hand, a particular ratio of resources available at city hospitals should be withheld for regular type patients as part of the tactical level decisions given at the beginning of each period of n days. These decisions, where resource allocations for regular patients are determined for each city hospital via the decision variables π_{hrt} (model **(D)**) and π^{ω}_{hrt} (model **(ASR)**), are given at every 10 days, i.e., on days $t \in \{1, 11, 21, 31, 41\}$, throughout the planning horizon. In this regard, to provide sufficient healthcare services to regular patients, the aggregated resources of the city hospitals withheld for treatments other than pandemic care should meet a particular ratio determined for each resource type $r \in R$. These ratios determined by the DMs for each resource type $r \in R$ are reported in Table 5.

Recall that in accordance with administrative rules, a new pandemic hospital can be opened only if the average number of patients allocated to the hospital of size $s \in S$ during the planning horizon is greater than the minimum level α_s. The values of these average utilization thresholds are determined as the 10% of the total bed capacities of different size pandemic hospitals by the DMs. Therefore, a small size pandemic hospital is installed provided that it accepts at least 40 patients on average during the planning horizon. Accordingly, the average utilization thresholds for medium and large size pandemic hospitals are determined as 120 and 180 patients, respectively.

5.2 The model (D) solution

In this section, we present the numerical results of the model **(D)**. We consider three objectives in the problem and these objectives are aggregated via linear scalarization to form a single objective in model **(D)**. Representing the importance of the objectives, these weights are inherently subjective and depend on the preference structure of the DM(s). Among the three approaches to elicit DM preferences and reflect them to the problem, namely, a priori, *interactive*, and a posteriori approaches, we employ a priori approach for solving the problem.

On the other hand, it may not be reasonable for the DM to provide these weights at the beginning of the problem-solving process without any knowledge about the problem structure. In this respect, we perform a posteriori weight analysis where we present solutions yielded by different weights to the DM as in the sensitivity analysis. To that end, we solved the model **(D)** for 66 different combination of weights such that $w_1, w_2, w_3 \in \{0.0, 0.1, \ldots, 0.9, 1.0\}$ and $w_1 + w_2 + w_3 = 1$. We implemented the model in General Algebraic Modeling System (GAMS 2012) and R (R Core Team 2017) and solved by CPLEX 12.5 with default settings. All runs are performed on a computer having Intel Xeon E5-2630 2.40 GHz (2 Core) processor and 128 GB of RAM. Based on the given data set, the model has 105,485 decision variables, 32 of which are discrete type and 35,740 constraints. CPU times of the solutions vary between 3.39 and 3672 s.

Computational runs yielded a total of 66 distinct solutions, i.e. none of the solutions obtained for a specific weight vector is dominated by another. Recall that Objective-1 represents the total number of patients that are rejected by hospitals due to capacity shortage. Essentially, this objective represents how much a solution is socially acceptable. Discussing with the DMs, it has been decided that any solution rejecting more than 15% of the total cases can not be referred to as a socially acceptable solution. Thus, we did not consider solutions (a total of 44) with a rejection percentage of 15% and more as applicable, and eliminated them from our solution set. The characteristics of the remaining 12 solutions are reported in Table 6.

In Table 6, columns 2–4 represent the weight combination used in the corresponding solution. We observe that the minimum weight of Objective-1 among all solutions is 0.5. This is in line with our previous decision regarding eliminating solutions having high rejection percentages. The following four columns report the aggregated and individual objective values of the solutions. The table is sorted in increasing order of the percentage of cases rejected that are listed in column nine. We observe that the minimum rejection percentage is 9.1% which corresponds to 4525 rejected cases in total during the 51 days long planning horizon. Note that the number of rejected cases not only depends on the number of hospital beds available at a particular period but also other sources that are consumed by patients based on the severity of their cases (ICU, non-ICU). This solution is yielded by the weight combination which gives the overall weight to the Objective-1 in the aggregated objective function, as expected. Among the 12 solutions, four of them suggest opening 22 new pandemic hospitals while four solutions suggest 23, two solutions suggest 20, one solution suggests 21, and one solution suggests 17, as reported in column 10. Column 11 reports the breakdown of the number of pandemic hospitals with respect to sizes. The first, second and third numbers separated with dashes represent the number of small ($s = 1$), medium ($s = 2$), and large ($s = 3$) size pandemic hospitals opened, respectively. It is worth noting that all solutions but solution 11 open 4 small pandemic hospitals. The number of medium size and large size hospitals opened varies in the range [8, 16] and [2, 7], respectively. The following column lists the particular location IDs of the suggested new pandemic hospitals. The last three columns report the ICU, nonICU, and total bed capacity acquired by opening the hospitals yielded by each solution.

In Table 7, we report the regret percentages of each solution's objective value with respect to the best value achieved for that particular objective. If we consider the Objective-1, for instance, solution 1 achieves the best (minimum) value among all 12 solutions, hence, its regret percentage is 0.0%. In this regard, this table assists the DMs to figure out how much regret will be accepted in each objective dimension if a particular solution is selected. The table reveals that regret percentages of Objective-1 are below 10% for the first eight solutions and increase dramatically after solution 9. In terms of Objective-2, there are relatively high

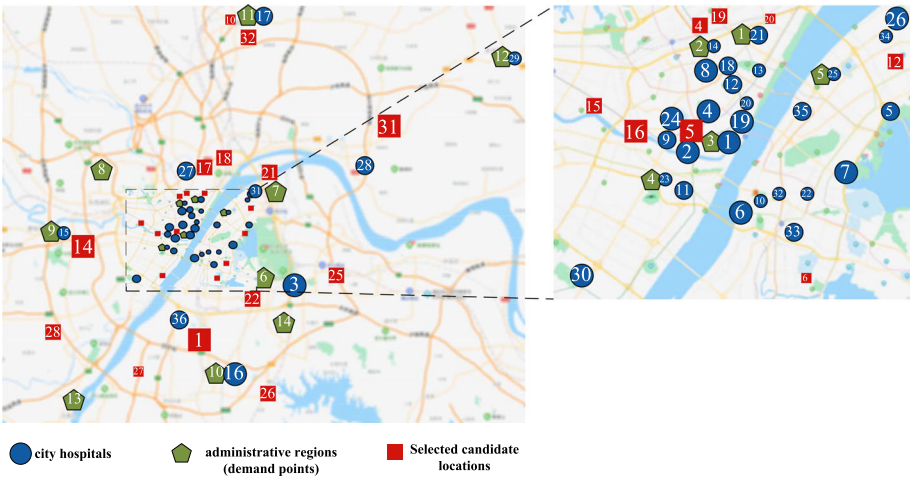

Fig. 5 Locations of the pandemic hospitals opened by the model **(D)**

regrets for solutions 1, 5, and 8, the values of which reach up to 414.7% while the rest vary between 0 and 44.5%. Other than the solution 12 that achieved the best figure in terms of Objective-3, the regret percentages of Objective-3 show relatively less dispersion and vary between the range [18.3%, 43.3%].

As we have also emphasised in Sect. 1, the problem we are tackling in this paper is related to public services and its outcome has a severe potential impact on the pandemic response management performance of governments. Therefore, the decisions tend to prioritize society benefits and seek for solutions that are *socially acceptable*. Conversely, this approach does not rule out other objectives such as cost since DMs also seek for solutions that are cost-effective. Considering all these aspects of the problem and in light of the a posteriori weight analysis, the DMs prefer choosing the solution 6 as the "most preferred" solution among 12 reported. This solution is generated by the weight set $\{0.8, 0.1, 0.1\}$ and puts special emphasis on Objective-1 which prioritize *society benefits* and proposes acceptable regrets for the remaining objectives. When this solution is implemented, the expected number of total rejected cases will be 4620, which is close to the minimum achievable value of 4525. In terms of Objective-2 that quantifies the total travel distance of people to allocated hospitals, solution 6 offers a fair and preferable solution when the average regret percentage in this objective is considered. This solution's relative regret percentage with respect to the best one is way below than the average value (44.4% vs. 115.4%). When the Objective-3 is considered, solution 6's relative regret percentage is less than the average relative regret and ranks fourth among 12 solutions reported. The locations of newly installed hospitals and their sizes are reported in Table 8 and displayed in Fig. 5. The solution suggests opening 4 small, 12 medium, and 5 large hospitals, yielding a total of 21 new pandemic hospitals in the Wuhan region.

Figure 6 shows the number of daily cases and the number of patients receiving treatment at city and pandemic hospitals. Recall that installation times of small, medium, and large size pandemic hospitals are taken as 4, 11, and 13 days, respectively. These times are indicated as vertical solid lines at those particular time periods in the figure. In this regard, the earliest time that pandemic hospitals start accepting patients is day five (the day after a small size hospital is built). The total number of patients receiving treatment at four small-sized pandemic hospitals is less than those receiving treatment at city hospitals until day 11. Once medium size

Table 6 Solutions having a rejection ratio less than 15%

Sol #	w_1	w_2	w_3	Obj. value	Φ_1	Φ_2	Φ_3	% Cases rejected	# of Open. Pand.Hos.	Opened sizes	Location IDs	Total ICU bed opened	Total nonICU bed opened	Total bed opened
1	1	0	0	0.10	4525	1,290,427	1,447,000	9.1	22	4-14-4	1-2-3-4-6-8-9-10-11-12-13-14-15-19-20-21-22-23-26-27-30-32	8400	16,800	25,200
2	0.9	0.1	0	0.12	4535	347,141	1,520,000	9.1	23	4-16-3	3-4-5-6-7-8-9-10-12- 13-15-16-17-18-19-20-21-23-26-27-28-30-32	8600	17,200	25,800
3	0.8	0.2	0	0.14	4562	342,637	1,517,000	9.1	23	4-16-3	3-4-5-6-7-8-9-10-12- 13-15-16-17-18-19-20-21-22-23-27-28-30-32	8600	17,200	25,800
4	0.7	0.3	0	0.15	4605	339,227	1,517,000	9.2	23	4-16-3	3-4-5-6-7-8-9-10-12- 13-15-16-17-18-19-20-21-22-23-27-28-30-32	8600	17,200	25,800
5	0.9	0	0.1	0.18	4606	1,408,023	1,289,000	9.2	20	4-9-7	1-2-6-10-14- 15-16-18-20-21-22-23-24-25-26-27-29-30-31-32	8200	16,400	24,600
6	0.8	0.1	0.1	0.20	4620	395,401	1,349,000	9.2	21	4-12-5	1-4-5-6-10-12-14- 15-16-17-18-19-20-21-22-25-26-27-28-31-32	8200	16,400	24,600
7	0.7	0.2	0.1	0.22	4654	361,125	1,392,000	9.3	22	4-15-3	3-4-5-6-7-8-10-12- 15-16-17-18-19-20-21-22-25-26-27-28-31-32	8200	16,400	24,600
8	0.8	0	0.2	0.25	4852	1,331,491	1,256,000	9.7	20	4-10-6	1-2-3-6-10-14-15- 16-18-20-21-22-24-25-26-27-29-30-31-32	8000	16,000	24,000
9	0.6	0.3	0.1	0.24	5429	309,315	1,401,000	10.9	22	4-16-2	3-4-5-6-7-8-10-12-13- 15-16-17-18-19-20-21-22-25-26-27-28-32	8000	16,000	24,000
10	0.6	0.4	0	0.17	5564	293,699	1,522,000	11.1	23	4-16-3	3-4-5-6-7-8-9-10-12-13- 15-16-17-18-19-20-21-22-23-26-27-28-32	8600	17,200	25,800
11	0.5	0.5	0	0.18	6228	273,573	1,499,000	12.5	22	3-16-3	3-4-5-6-7-8-9-10-12-13-15-16-17-18-19-20-21-22-23-26-28-32	8500	17,000	25,500
12	0.7	0.1	0.2	0.28	6856	383,264	1,062,000	13.7	17	4-8-5	1-5-6-10-12-14-15-16-18-19-20-21-22-25-27-31-32	6600	13,200	19,800

Table 7 Regrets of objective values with respect to the best ones **(D)**

Sol #	w_1	w_2	w_3	% Regret		
				Φ_1	Φ_2	Φ_3
1	1	0	0	0.0	371.7	36.3
2	0.9	0.1	0	0.2	26.9	43.1
3	0.8	0.2	0	0.8	25.2	42.8
4	0.7	0.3	0	1.8	24.0	42.8
5	0.9	0	0.1	1.8	414.7	21.4
6	0.8	0.1	0.1	2.1	44.5	27.0
7	0.7	0.2	0.1	2.9	32.0	31.1
8	0.8	0	0.2	7.2	386.7	18.3
9	0.6	0.3	0.1	20.0	13.1	31.9
10	0.6	0.4	0	23.0	7.4	43.3
11	0.5	0.5	0	37.6	0.0	41.1
12	0.7	0.1	0.2	51.5	40.1	0.0
Average				12.4	115.5	31.6

Table 8 Locations and sizes of the pandemic hospitals opened by the model **(D)**

Size	Location IDs
Small ($s = 1$)	6-10-20-27
Medium ($s = 2$)	4-12-15-17-18-19-21-22-25-26-28-32
Large ($s = 3$)	1-5-14-16-31

pandemic hospitals become operational at day 12, the burden of pandemic patient treatment is taken over by them. The number of daily cases increases gradually and reaches its peak point at day 17 with 13,436 daily confirmed cases. This dramatic increase at day 17 is compensated by the large size hospitals that become operational at day 14. The relief provided by these new large pandemic hospitals can clearly be observed through the sudden increase in the number of patients receiving treatment at pandemic hospitals from 5304 at day 16 to 17,291 at day 17. After day 17, the number of daily cases decreases dramatically and finally vanishes by day 51.

Figure 7 presents the number of daily cases as well as the number of cases rejected by hospitals due to capacity shortages. As can be seen from the figure, the number of rejected cases increases until day nine and decreases gradually until day 12. This pattern is in harmony with the temporary decrease in the number of cases between days 9 and 11. On the other hand, even though the number of cases increases again at day 12, the number of rejected cases decreases to zero thanks to the newly opened 12 medium-size hospitals at that day. After this time till the end of day 51 where the number of cases vanishes, none of the cases is rejected except for day 18 where a total of 82 cases (corresponding to 2.1% of confirmed cases at day 18) are rejected primarily due to the dramatic increase in the number of cases at day 17. As we have emphasised before, this peak is compensated by the five large size hospitals that become operational as of day 14. Throughout the planning horizon, the total number of rejected cases is 4620. Majority of these cases are those that are rejected at the early stage of the pandemic, between days 4–12 due to the cumulative increase in the number of patients receiving pandemic treatment at hospitals. During these early days of the pandemic, the construction of medium and large size hospitals are still in progress. Even though it would be

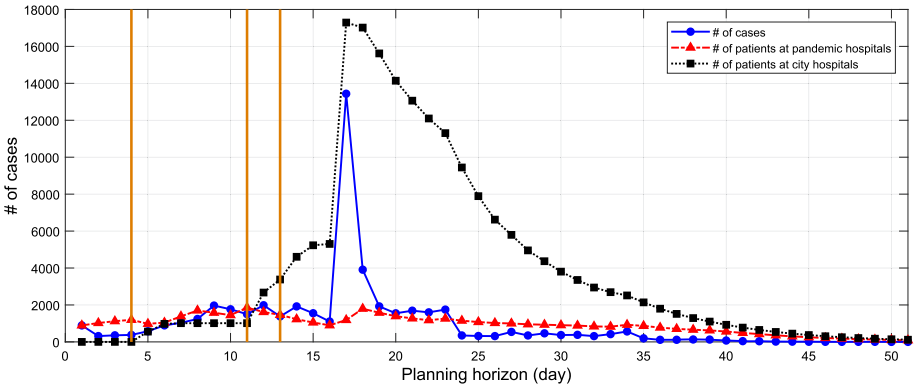

Fig. 6 The number of daily cases and number of patients receiving treatment at city hospitals and pandemic hospitals

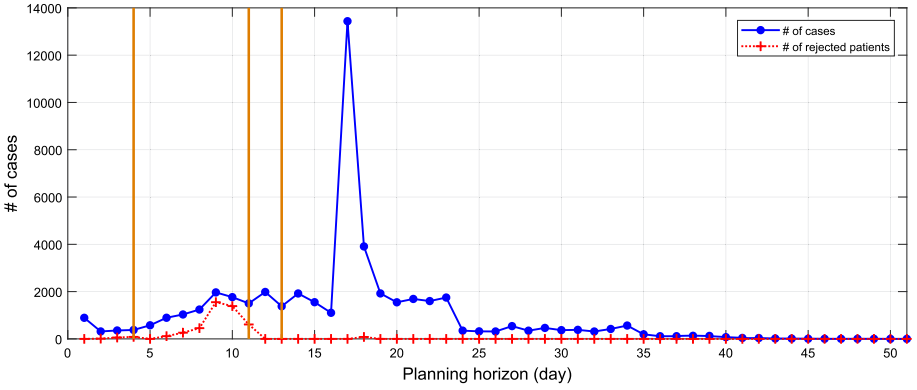

Fig. 7 Number of daily cases and number of cases rejected

possible to meet all the demand during the early stage cases by opening all hospitals of small size, this decision would lead to more rejected cases at later stages of the pandemic where daily cases increase dramatically. Aiming to minimize the total number of rejected cases throughout the planning horizon, model **(D)** ventures on rejecting early stage cases in return for low average rejection rates throughout the planning horizon. These observations indicate that the most important parameter among the problem data are the installation times of the hospitals. The earlier the new pandemic hospitals are installed, the less cases are rejected due to capacity shortage.

Besides these strategic decisions, model **(D)** also yields tactical and operational decisions which correspond to resource allocation among healthcare facilities and patient allocation of districts to the hospitals. To illustrate tactical decisions yielded by the model **(D)**, we report ratios of resources allocated to pandemic patients at different time periods from each city hospital in Table 14. Recall that tactical decisions are made every ten days, hence, the ratios of resources allocated are determined at days $\{1, 11, 21, 31, 41\}$. In Table 14, rows correspond to the city hospitals and rows correspond to the allocation ratios of resources.

Having all these aforementioned properties, solution 6 provides a compromise solution with respect to the three objectives and presents a *socially acceptable* course of action for providing fair and adequate healthcare services to the society during the pandemic.

5.3 The model (ASR) solution

The solution of the model **(D)** is based on only one scenario that is forecasted to happen. There are many studies in the recent literature that propose techniques to forecast the number of confirmed cases for a pandemic, however, these techniques are out of the scope of this study. Conversely, forecasting techniques inherently involve uncertainty due to the parameters assumed or estimated, such as the spread speed of the pandemic or the time, extent, and efficiency of the government policies to respond to the pandemic. These uncertainties affect the daily number of cases and duration of the pandemic. In this respect, the obtained solution should be robust to the possible scenarios that may happen. Our **(ASR)** model addresses this phenomenon and considers multiple scenarios simultaneously while obtaining solutions that keep the relative regret for each scenario under a predefined threshold. To illustrate the applicability of the **(ASR)** model, we generate seven scenarios, one of which is the baseline scenario we employed in Sect. 5.2. Without loss of generality, we generated the rest of the scenarios by applying perturbations to the confirmed daily cases of each district of the baseline scenario. On the other hand, we would like to emphasize that the model **(ASR)** is flexible to incorporate different number of scenarios having different durations, start times, and patterns. The applied perturbations vary in the range $\{-15\%, -10\%, \ldots, 10\%, 15\%\}$.

Firstly, all generated scenarios are solved with model **(D)** by using the same weight combination that we determined in Sect. 5.2. Information regarding these seven scenarios and their optimal solutions are given in Table 9. Note that scenario 4 corresponds to the baseline scenario. Columns two and three represent the perturbation levels and the resulting total number of confirmed cases of scenarios, respectively. The next four columns report the objective function values of scenarios. Optimal solutions suggest opening different number and sizes of pandemic hospitals for each scenario. The solution of the most demanding scenario (scenario 7) opens 24 new pandemic hospitals, while in the least demanding scenario (scenario 1) 18 hospitals are opened. One remarkable observation in Table 9 is that opening four small size pandemic hospitals is dictated by all scenarios simultaneously.

After obtaining the optimal objective values of the individual scenarios which correspond to $\xi^{\omega *}$ parameters of the **(ASR)** model, we first solve the model by removing constraints (26). Without loss of generality, we assume that all scenarios have equal occurrence probabilities even though other probability distributions can be applied based on expert opinion or further analysis. When the contraints (26) are removed, the model **(ASR)** is essentially a stochastic programming model that minimizes the total expected objective value across all seven scenarios. This initial step enables us to obtain an initial upper bound on the relative regrets (τ^{ω}) of individual scenarios. Based on this current upper bound, the relative regret threshold is determined and the model is solved iteratively by employing the procedure given in Fig. 2. Different scaling factors (ζ) are experimented in the procedure and a scaling factor of 0.97 is determined as the final value since it provides tighter bounds. The procedure runs and generates solutions for two iterations until the model **(ASR)** becomes infeasible at the third iteration. In Table 10 the columns tree and four report the objective values and relative regrets of the individual scenarios in the initial solution of **(ASR)**, respectively. The last two columns show the progress of relative regrets of the scenarios at each iteration. Note that the upper bound on the relative regrets are indicated with a bold font in each column. Table 10

Table 9 Optimal solutions of scenarios obtained by solving model **(D)**

Scen.	Perturb. (%)	# of total cases	Obj. val.	Φ_1	Φ_2	Φ_3	# of Open. Pand.Hosp.	Opened sizes	Location IDs
1	− 15.00	41,869	0.179	2985	346,327	1,141,000	18	4-9-5	1-4-5-6-10-12-14-15-16-18-19-20-21-22-25-27-31-32
2	− 10.00	44,359	0.192	3461	360,872	1,212,000	19	4-10-5	1-4-5-6-10-12-14-15-16-17-18-19-20-21-22-25-27-31-32
3	− 5.00	46,772	0.196	3922	379,142	1,278,000	20	4-11-5	1-4-5-6-10-12-14-15-16-17-18-19-20-21-22-25-26-27-31-32
4	0.00	49,988	0.203	4620	395,401	1,349,000	21	4-12-5	1-4-5-6-10-12-14-15-16-17-18-19-20-21-22-25-26-27-28-31-32
5	5.00	53,204	0.210	5170	393,668	1,477,000	23	4-15-4	1-3-4-5-6-7-8-10-12-15-16-17-18-19-20-21-22-25-26-27-28-31-32
6	10.00	55,617	0.212	5632	428,504	1,526,000	23	4-13-6	1-4-5-6-7-8-10-12-14-15-16-17-18-19-20-21-22-25-27-28-29-31-32
7	15.00	58,107	0.217	6129	437,229	1,605,000	24	4-14-6	1-3-4-5-6-7-8-10-12-14-15-16-17-18-19-20-21-22-23-25-27-28-31-32

Table 10 Initial and iterative τ^{UB} values

Scenario	$\xi^{\omega*}$	ξ^{ω}	τ^{ω} (%)	τ_1^{ω} (%)	τ_2^{ω} (%)
1	0.179	0.194	**8.53**	**7.45**	7.07
2	0.192	0.202	5.47	4.42	4.60
3	0.196	0.201	2.47	1.59	1.72
4	0.203	0.203	0.20	1.05	1.11
5	0.210	0.214	2.05	3.33	3.55
6	0.212	0.221	4.43	5.76	5.72
7	0.217	0.230	6.11	7.33	**7.13**

reveals that the more perturbation a scenario has, the more regret is borne for that scenario. As expected, the model **(ASR)** makes the trade-off between the total number of rejected patients and the total cost of opening new pandemic hospitals.

Table 11 reports the solutions generated by the model **(ASR)** through iterations. The second column shows the regret upper bounds of each solution. The last column reports the difference between the present solution and the previous one. As the relative regret threshold is shrunk, the objective value worsens as expected because the constraints (26) get tighter. The initial solution opens 21 new pandemic hospitals with 4 small, 12 medium, and 5 large sizes. In the first iteration following the initialization, the large size pandemic hospital at location 1 is closed and a medium size pandemic hospital is opened at location 28, while the total number of open pandemic hospitals remains unchanged. In the second iteration pandemic hospitals at locations 8 (medium), 14 (large), and 28 (medium) are closed and hospitals at location 1 (large), 3 (medium), and 7 (medium) are opened. At iteration three the model **(ASR)** becomes infeasible and the procedure stops by yielding the solution of iteration two as the optimal solution.

Objective functions' progress through iterations are presented in Table 12. We observe that the Objective-1 values (total number of rejected patients) of the individual scenarios get worse at iteration one due to closing a large size hospital and opening a medium size hospital instead. Since the number and size of the opened hospitals remains the same at iteration two, the Objective-1 values of the individual scenarios do not change. Conversely, the Objective-2 values (total walking distances of patients) of the scenarios improve at iteration one while worsen at iteration two. The Objective-3 values (total installation costs of new pandemic hospitals) improve steadily until the model gets infeasible. This observation indicates that the upper bounds on regrets are generally driven by the Objective-3.

Consequently, the sizes and locations of the newly installed hospitals yielded by model **(ASR)** are given in Table 13 and shown visually in Fig. 8. Even though this solution opens 21 new pandemic hospitals as also yielded by model **(D)**, model **(ASR)** opens four large pandemic hospitals instead of five and 13 medium size hospitals instead of 12. By making this size modification, the model **(ASR)** reduces installation costs in return for an increase in total walking distance and total number of rejected patients to keep the individual regrets of the scenarios under a predefined threshold.

5.4 Discussion

Model **(D)** relies on a deterministic forecasted data of daily confirmed cases of each demand (population) center. Based on this forecasted data, our model finds solutions for strategic,

Table 11 Solution progress through iterations

Iter.	τ^{UB}	Obj. val	# of Op. P. Hosp.	Opened sizes	Locations opened	Difference in solution
Init.	8.53%	0.209	21	4-12-5	1-4-5-6-8-10-12-14-15-16-17-18-19-20-21-22-25-26-27-31-32	–
1	7.45%	0.210	21	4-13-4	4-5-6-8-10-12-14-15-16-17-18-19-20-21-22-25-26-27-28-32-32	1(L) closed 28(M) opened
2	7.13%	0.210	21	4-13-4	1-3-4-5-6-7-10-12-15-16-17-18-19-20-21-22-25-26-27-31-32	8(M), 14(L), 28(M) closed 1(L), 3(M), 7(M) opened
3	–	Infeasible				–

Table 12 Objective functions' progress through iterations

	Obj.	Φ_1			Φ_2			Φ_3		
	Iter.	Init	1	2	Init	1	2	Init	1	2
Scenario	1	2984	2986	2986	338,379	328,656	340,546	1,361,000	1,347,000	1,323,000
	2	3461	3463	3463	349,819	339,238	362,145			
	3	3913	3917	3917	363,876	354,451	377,578			
	4	4620	4871	4871	386,763	375,023	395,789			
	5	5865	6149	6149	395,593	380,849	405,489			
	6	6928	7213	7213	402,696	389,776	409,587			
	7	8036	8322	8322	410,712	397,283	410,515			

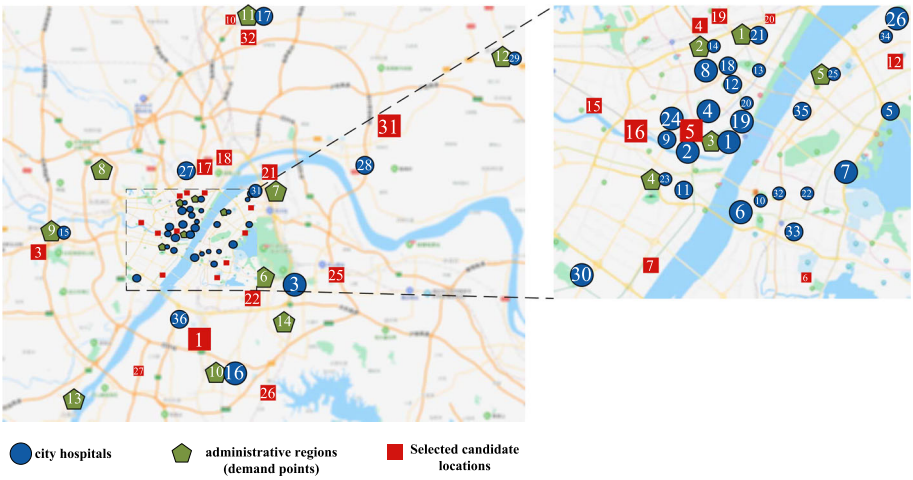

Fig. 8 Locations of the pandemic hospitals opened by the model **(ASR)**

Table 13 Locations and sizes of the pandemic hospitals opened by the model **(ASR)**

Size	Location IDs
Small ($s = 1$)	6-10-20-27
Medium ($s = 2$)	3-4-7-12-15-17-18-19-21-22-25-26-32
Large ($s = 3$)	1-5-16-31

tactical, and operational decisions. Even though the uncertainties associated with the forecasted data make it challenging to make strategic decisions, these type of decisions should be given rapidly to respond to the pandemic. Because the realization of these decisions such as construction of new hospitals takes time and they should be given on the early stages of the pandemic.

When a pandemic emerges, the policy makers do not have the convenience to wait for reliable empirical data, conversely, have to rely on limited information about model parameters and system states, which is derived from expert options, incomplete field assessment, and historical data (Du et al. 2020). Moreover, pandemic/epidemic outbreaks also inspire local and global collaboration among researchers, policy makers and practitioners with a view to devise strategies, disease spread models and actions on how to address the outbreak (Cronjé 2019).

As the numerical analysis of the case study reveals, the long-term decisions made in the initial days of the pandemic have a dramatical impact on improving the preparedness level of the healthcare system. Hence, the lack of complete information in the early phases of a pandemic does not rule out the necessity to make long-term decisions at the beginning. In order to hedge against the uncertainty inherent in pandemics, many researchers propose breaking down the planning horizon into manageable terms (levels) such as short, medium, and long terms where upper level decisions can be tailored at the beginning of each level in the light of additional information and empirical data obtained thus far (Savachkin and Uribe 2012; Long et al. 2018; Nikolopoulos et al. 2020). In this study, we adopt the same strategy by considering three decision types, each of which corresponds to different decision levels having different time spans, namely, (*i*) strategic (opening new pandemic hospitals and their

size), (*ii*) tactical (allocation of resources among healthcare facilities), and (*iii*) operational (allocation of patients to hospitals). Our solution approach provides the flexibility to rerun the model at the beginning of these decision periods with additional empirical information and tailor subsequent decisions.

In order to hedge against the uncertainty inherent in the pandemic data, our *p*-robust model **(ASR)** considers multiple scenarios simultaneously. For illustrative purposes, we employed scenarios that are obtained by applying perturbations to the baseline scenario's daily confirmed cases. However, the model **(ASR)** can handle various scenarios having different (number of) peaks (shapes) and different durations. Even though there exist other robust modeling techniques such as the utilization of uncertainty sets for the parameters, note that the uncertainties associated with the confirmed case data can not be solely confined to the uncertainties of problem parameters. For instance, the lock-down and opening decisions of governments affect the spread pattern of the pandemic and changes the number of daily cases dramatically. The time and extent of these measures are determined by governments based on the course of the pandemic. Additionally, the development of a new cure and vaccine or mutation of the virus which leads to a higher spread speed may have dramatic impacts on the shape and the duration of the forecasted data. In this respect, we believe that employing *p*-robustness concept that considers multiple distinct scenarios within a decision model is an appropriate way to handle uncertainties in problems involving forecasted data of the pandemic.

Among problem parameters, the installation times of different size hospitals have the most significant impact on the number of rejected patients. Essentially, candidate locations and relevant sizes have enough capacity to serve all pandemic patients along with city hospitals. In other words, if the new pandemic hospitals were available at day one, then none of the pandemic patients would be rejected even in the most demanding scenario (Scenario-7). Therefore, the most important decision parameter that should be focused is the installation times of the hospitals. To that end, opening hospitals with partial capacities while the construction still continues might reduce the number of rejected pandemic patients and provide a socially acceptable course of action.

6 Conclusion

In this study, we consider the problem of health resource management and location allocation problem during the early stages of pandemic/epidemic under demand uncertainty. This problem is particularly important because failing to respond to the pandemic rapidly and efficiently may cause noncompensable suffering for the society. Being one of the most essential tasks of a social government, the public health should be safeguarded with effective measures determined through analytical decision making processes. Hence, in this research, our main purpose is to improve the preparedness level and response effectiveness of healthcare authorities in responding pandemics/epidemics by implementing operations research techniques.

We can briefly summarize the contribution of the study as follows: First, our novel modeling approach incorporates strategic, tactical, and operational decisions into a single decision model. This approach provides extensive flexibility to healthcare authorities for efficient resource allocation. Moreover, these tactical and operational decisions can be tailored during the planning horizon by rerunning the model based on the new data available. Second, our multi-objective model and a posteriori weight analysis enable DMs to reflect their preferences

regarding the objectives in an efficient way. With this approach, the DMs can get acquainted with the problem structure and observe the impacts of their preferences on the solution. Third, employing the *p*-robustness concept, our robust model can handle multiple scenarios that may have differences in terms of spread speed, duration and shape simultaneously by keeping the relative regret of individual scenarios under a predefined threshold. Our robust modeling approach provides socially acceptable solutions and hedges against uncertainty in an efficient way.

We also would like to recall that our proposed model incorporates three conflicting objectives that seek to minimize (*i*) the number of patients rejected by hospitals, (*ii*) travel distance of patients and (*iii*) the installation cost of new pandemic hospitals. Note that, the first objective is a *socially-driven* term which basically attempts to improve the health service quality by suggesting the installation of several large pandemic hospitals and allocation of sufficient resources to patients. Similarly, the second objective drives planners to install relatively small size pandemic hospitals in large numbers close to demand centers to minimize the travel distance of patients. Since solutions imposed by these two objectives explicitly contribute toward additional financial burdens being placed on the health system, they naturally conflict with the third objective, i.e. the cost term.

Considering that our research topic is strictly related to public services in terms of creating an impact on the quality of the pandemic response of governments, we did not consider solutions with rejection ratios larger than a specific threshold, i.e. a ratio of 15%, feasible. Although with this special emphasis on the first objective we impose a positive discrimination to socially acceptable solutions, we do not rule out other solutions that incorporate financial considerations of DMs. To be more specific, the suggested a posteriori weight analysis approach allows DMs choose their most preferred solution among all non-dominated alternatives with varying objective terms and regret values.

Adapting the weights preferred by the DMs via the a posteriori weight analysis, the robust model **(ASR)** generates a solution that prescribes the total number of rejected patients (4th column) and total travel distances (7th column) given in Table 12 for each scenario with a total installation cost of 1,323,000 ¥, by opening 4 small, 13 medium, and 4 large size hospitals the locations of which are shown in Fig. 8.

Our study has some theoretical implications. The extent of spread speed and transmission as well as the severity of the disease may be unclear during the early stages of a pandemic. Thus, to account for the demand uncertainty and attain a more socially acceptable solution, robust optimization approach provides efficient modeling techniques. Using robust optimization might help DMs to avoid noncompensable regrets once the veil of uncertainty disappears. As another theoretical implication, in order to hedge against the uncertainty inherent in pandemics, breaking down the planning horizon into manageable terms (levels) such as short, medium, and long terms and building the mathematical model accordingly provides the flexibility to the DMs in terms of tailoring the upper level decisions in the light of additional information and empirical data obtained thus far.

The most important practical implication of this study is that, once a pandemic emerges, prompt decisions should be made by the DMs to alleviate the human suffering and improve the health system preparedness. Our study has shown that the installation times of different size hospitals have the most significant impact on the number of rejected patients. In this respect, even though there exist scarce empirical data at the early stage of the pandemic, long-term decisions should be made based on expert options, incomplete field assessment, and historical data. Moreover, opening hospitals with partial capacities while the construction still continues might reduce the number of rejected pandemic patients and provide a socially acceptable course of action.

This study has two limitations. Firstly, even though forecasting the daily confirmed cases is out of scope of this study, the accuracy of the forecasted data is important for particularly strategic decisions. Secondly, if the problem size increases due to an increase in number of population centers, candidate locations for new pandemic hospitals, and scenarios, then efficient solution techniques such as heuristics, meta-heuristics might be required to solve the problem in reasonable CPU times.

There are two potential research directions that can be addressed as future work. One research direction is to solve the model **(D)** with other multi-objective solution approaches. In this work, we utilized the linear scalarization approach to aggregate the objective functions. Instead of a scalarization approach, *interactive* approaches where the DM interacts with the method for searching the most preferred solution or a posteriori approaches where a Pareto frontier is presented to the DM can be used to solve the problem. When the DM does not have a clear idea of the problem's mathematical structure, then the problem consists not only of finding the best method to apply to DM's problem but also establishing a representation of the problem in a constructive way (Erişkin 2021). In these cases, the *interactive* approaches are particularly useful. Another research direction is to generate more realistic scenarios via simulations that reflect the impacts of pandemic related decisions such as lock-down and opening, and other pandemic related inputs such as immunization campaigns and a newly developed cure, and then to solve the model **(ASR)** incorporating these scenarios.

Acknowledgements The authors did not receive any specific grant from funding agencies in the public, commercial, or non-profit sectors.

Declarations

Conflict of interests The authors declare that they have no conflict of interest.

Disclaimer The views and conclusions contained herein are those of the authors and should not be interpreted as necessarily representing the official policies or endorsements, either expressed or implied, of any affiliated organization or government.

Appendix

See Table 14.

Table 14 Ratio of resources allocated to pandemic patients at different time periods from each city hospital

h	ICU bed					Non-ICU bed				
	$t \in [1, 10]$	$t \in [11, 20]$	$t \in [21, 30]$	$t \in [31, 40]$	$t \in [41, 50]$	$t \in [1, 10]$	$t \in [11, 20]$	$t \in [21, 30]$	$t \in [31, 40]$	$t \in [41, 50]$
1	1.000	1.000	0.442	0.572	0.582	0.162	0.133	1.000	0.116	1.000
2	1.000	0.048	0.048	1.000	1.000	0.077	0.082	0.052	0.072	1.000
3	0.752	1.000	1.000	1.000	1.000	0.045	0.064	1.000	0.040	1.000
4	1.000	1.000	0.366	1.000	0.168	0.025	0.027	1.000	0.025	1.000
5	1.000	1.000	1.000	1.000	1.000	0.235	0.251	0.213	0.199	0.788
6	0.480	0.080	0.054	0.981	1.000	1.000	1.000	1.000	1.000	1.000
7	1.000	1.000	0.281	1.000	0.013	0.056	1.000	0.048	0.005	1.000
8	0.166	0.178	0.178	0.329	0.313	0.222	0.134	0.130	1.000	1.000
9	1.000	0.625	0.624	1.000	0.721	0.193	1.000	0.110	0.056	1.000
10	1.000	0.803	0.724	0.157	0.026	0.105	1.000	0.055	0.005	1.000
11	1.000	1.000	1.000	0.288	0.049	0.384	0.400	0.271	0.021	1.000
12	1.000	0.519	1.000	0.630	1.000	0.391	0.405	0.320	0.050	1.000
13	1.000	0.909	0.909	0.970	1.000	0.597	0.558	0.413	0.388	1.000
14	0.564	1.000	1.000	1.000	1.000	0.599	0.684	0.508	0.485	1.000
15	1.000	1.000	1.000	1.000	0.887	1.000	0.283	0.282	0.170	1.000
16	1.000	0.661	0.728	1.000	0.454	0.200	0.193	0.192	0.086	1.000
17	1.000	0.909	0.908	0.987	1.000	0.169	1.000	0.142	0.160	0.075
18	1.000	1.000	0.936	1.000	0.416	0.127	0.134	0.123	1.000	1.000
19	0.437	0.393	0.270	1.000	0.109	0.045	0.049	0.049	0.052	1.000
20	1.000	1.000	1.000	0.385	0.064	0.228	0.235	0.159	0.029	1.000
21	0.000	0.000	0.000	0.000	0.000	0.000	0.000	0.000	0.000	0.000
23	1.000	0.400	0.400	0.407	1.000	0.261	0.313	0.178	0.194	1.000
24	1.000	1.000	1.000	0.387	0.066	0.483	0.420	0.239	0.018	0.002
25	1.000	0.622	0.623	0.623	0.842	0.358	0.214	1.000	0.209	1.000

Table 14 continued

h	ICU bed					Non-ICU bed				
	$t \in [1, 10]$	$t \in [11, 20]$	$t \in [21, 30]$	$t \in [31, 40]$	$t \in [41, 50]$	$t \in [1, 10]$	$t \in [11, 20]$	$t \in [21, 30]$	$t \in [31, 40]$	$t \in [41, 50]$
26	1.000	0.562	0.562	0.596	0.609	0.166	0.140	0.129	0.129	0.085
27	1.000	1.000	0.701	1.000	1.000	0.234	0.174	0.071	0.006	1.000
28	1.000	0.657	0.447	0.067	1.000	0.111	0.111	0.020	0.003	0.001
29	1.000	1.000	0.093	1.000	1.000	0.195	0.194	1.000	0.005	1.000
32	1.000	0.909	1.000	0.347	0.059	0.401	0.391	0.260	0.021	1.000
33	0.091	0.227	0.249	0.200	0.222	0.141	0.122	0.076	0.020	1.000
34	0.000	0.000	0.000	0.000	0.000	0.000	0.000	0.000	0.000	0.000
35	0.000	0.000	0.000	0.000	0.000	0.000	1.000	0.000	0.000	0.000
36	1.000	0.606	0.606	0.207	0.036	1.000	0.965	0.548	0.041	1.000
h	Doctor					Nurse				
	$t \in [1, 10]$	$t \in [11, 20]$	$t \in [21, 30]$	$t \in [31, 40]$	$t \in [41, 50]$	$t \in [1, 10]$	$t \in [11, 20]$	$t \in [21, 30]$	$t \in [31, 40]$	$t \in [41, 50]$
1	0.230	0.211	1.000	0.200	0.164	1.000	0.296	0.288	0.285	1.000
2	1.000	1.000	1.000	0.065	1.000	0.099	0.115	0.086	0.106	1.000
3	0.061	0.090	1.000	0.065	1.000	1.000	0.119	0.085	1.000	1.000
4	0.054	0.055	1.000	1.000	1.000	1.000	1.000	1.000	1.000	1.000
5	0.287	0.325	0.290	0.277	1.000	0.868	1.000	0.900	0.865	1.000
6	1.000	0.030	1.000	1.000	1.000	1.000	1.000	0.685	0.103	1.000
7	0.097	0.107	0.092	0.020	1.000	0.264	0.283	0.254	0.060	1.000
8	0.154	0.123	0.122	1.000	1.000	1.000	0.225	0.223	0.223	1.000
9	0.383	0.421	0.283	0.172	1.000	1.000	0.190	1.000	0.083	1.000
10	0.225	0.239	0.160	0.023	1.000	1.000	0.232	0.165	0.026	1.000
11	0.267	0.269	0.213	1.000	1.000	1.000	1.000	0.815	0.127	1.000
12	0.147	0.158	0.134	0.044	1.000	1.000	0.131	0.113	0.042	0.013

Table 14 continued

h	Doctor					Nurse				
	$t \in [1, 10]$	$t \in [11, 20]$	$t \in [21, 30]$	$t \in [31, 40]$	$t \in [41, 50]$	$t \in [1, 10]$	$t \in [11, 20]$	$t \in [21, 30]$	$t \in [31, 40]$	$t \in [41, 50]$
13	0.311	0.325	0.264	0.252	1.000	0.617	0.664	0.548	0.526	1.000
14	0.492	0.597	0.485	0.469	0.350	0.580	0.713	0.590	0.572	1.000
15	0.865	0.851	0.844	0.593	1.000	0.678	0.671	0.665	0.480	1.000
16	0.204	0.203	0.203	0.122	1.000	1.000	1.000	1.000	0.630	1.000
17	0.132	1.000	1.000	0.127	1.000	0.573	0.742	0.516	0.556	0.362
18	0.123	1.000	0.123	1.000	1.000	1.000	1.000	1.000	1.000	1.000
19	1.000	1.000	0.037	1.000	1.000	1.000	1.000	1.000	1.000	0.396
20	0.399	1.000	0.381	0.106	0.016	1.000	1.000	1.000	1.000	1.000
21	0.000	0.000	0.000	0.000	0.000	0.000	0.000	0.000	0.000	0.000
23	0.671	0.842	0.566	0.600	1.000	1.000	0.172	0.120	0.126	1.000
24	0.171	0.170	0.114	0.018	1.000	0.626	0.642	0.446	0.077	0.012
25	0.462	0.369	0.366	0.366	0.359	0.432	0.368	0.366	0.366	0.361
26	0.143	0.139	0.137	0.137	0.105	1.000	1.000	1.000	1.000	0.788
27	0.201	0.186	0.111	1.000	1.000	1.000	0.967	0.614	0.095	1.000
28	0.100	0.100	0.061	0.009	0.001	1.000	1.000	0.685	0.104	0.016
29	0.636	0.635	0.317	0.048	1.000	0.155	0.155	0.086	0.013	1.000
32	0.392	0.388	0.306	0.050	0.007	0.394	0.391	0.319	0.057	0.009
33	0.240	1.000	0.162	0.066	1.000	0.267	0.272	0.190	0.084	0.061
34	0.000	0.000	0.000	0.000	0.000	0.000	0.000	0.000	0.000	0.000
35	0.000	0.000	0.000	0.000	0.000	0.000	0.000	0.000	0.000	0.000
36	0.300	0.325	0.219	1.000	1.000	1.000	0.724	0.504	0.079	1.000
h	Lab Technician					ECMO				
	$t \in [1, 10]$	$t \in [11, 20]$	$t \in [21, 30]$	$t \in [31, 40]$	$t \in [41, 50]$	$t \in [1, 10]$	$t \in [11, 20]$	$t \in [21, 30]$	$t \in [31, 40]$	$t \in [41, 50]$
1	0.105	1.000	0.105	0.105	0.097	0.155	0.164	0.165	0.214	0.217
2	0.039	1.000	1.000	0.045	0.023	0.030	0.045	0.045	0.052	0.049

Table 14 continued

h	Lab Technician					ECMO				
	$t \in [1, 10]$	$t \in [11, 20]$	$t \in [21, 30]$	$t \in [31, 40]$	$t \in [41, 50]$	$t \in [1, 10]$	$t \in [11, 20]$	$t \in [21, 30]$	$t \in [31, 40]$	$t \in [41, 50]$
3	0.115	1.000	1.000	1.000	0.112	0.075	0.100	0.100	0.100	0.100
4	1.000	1.000	0.022	0.020	0.012	0.098	0.089	0.091	0.066	0.042
5	0.162	1.000	0.178	1.000	0.085	0.052	0.083	1.000	0.083	0.083
6	0.014	0.013	1.000	1.000	0.000	0.131	0.116	1.000	0.011	1.000
7	0.034	1.000	0.034	1.000	0.001	0.132	1.000	1.000	0.046	0.007
8	0.067	0.067	0.067	0.067	0.060	0.077	0.083	0.083	1.000	0.146
9	0.087	1.000	1.000	0.052	0.042	0.041	0.083	0.083	0.101	0.096
10	0.381	0.381	0.310	0.052	0.008	0.141	1.000	1.000	0.022	0.004
11	0.130	0.130	0.110	0.020	0.003	0.133	0.133	0.133	0.038	0.007
12	0.098	0.108	0.096	0.047	0.014	0.053	0.060	0.071	0.073	0.023
13	0.138	0.159	0.137	0.133	0.092	0.027	0.060	1.000	0.064	0.066
14	0.139	1.000	0.153	0.149	0.119	0.047	1.000	0.083	0.083	0.083
15	0.995	1.000	0.989	0.761	0.485	0.091	0.108	0.108	0.108	0.096
16	0.100	0.100	0.100	0.069	0.038	1.000	0.121	0.133	0.135	0.083
17	0.095	0.116	0.088	0.093	0.067	0.074	0.075	1.000	0.082	0.083
18	0.056	0.056	0.055	0.055	0.021	0.133	1.000	0.124	0.133	1.000
19	0.025	0.024	1.000	0.020	0.009	0.196	0.176	0.121	0.089	0.049
20	1.000	0.885	0.885	0.278	0.044	0.199	0.199	0.199	0.077	0.013
21	0.000	0.000	0.000	0.000	0.000	0.000	0.000	0.000	0.000	0.000
23	0.101	1.000	0.099	0.103	0.089	0.049	0.083	1.000	0.085	0.089
24	0.337	1.000	0.283	0.058	0.009	0.004	0.011	0.011	1.000	0.001
25	0.088	0.088	0.088	0.088	0.088	0.078	1.000	1.000	0.083	0.112
26	0.107	0.107	0.107	0.107	0.090	0.098	1.000	0.098	1.000	0.106

Table 14 continued

h	Lab Technician					ECMO				
	$t \in [1, 10]$	$t \in [11, 20]$	$t \in [21, 30]$	$t \in [31, 40]$	$t \in [41, 50]$	$t \in [1, 10]$	$t \in [11, 20]$	$t \in [21, 30]$	$t \in [31, 40]$	$t \in [41, 50]$
27	0.086	0.086	0.061	0.010	0.002	0.076	1.000	0.093	1.000	1.000
28	0.062	0.078	0.053	0.008	0.001	0.033	1.000	1.000	0.009	1.000
29	0.190	0.190	0.131	0.020	0.003	1.000	1.000	1.000	1.000	0.003
32	0.489	0.489	0.431	0.090	0.014	0.067	1.000	1.000	0.029	0.005
33	0.052	0.058	0.043	0.022	0.018	0.012	1.000	1.000	0.027	0.029
34	0.000	0.000	0.000	0.000	0.000	0.000	0.000	0.000	0.000	0.000
35	0.000	0.000	0.000	0.000	0.000	0.000	0.000	0.000	0.000	0.000
36	0.181	0.218	0.164	1.000	0.005	0.038	0.091	0.090	1.000	0.005
h	Tomography					Ventilator				
	$t \in [1, 10]$	$t \in [11, 20]$	$t \in [21, 30]$	$t \in [31, 40]$	$t \in [41, 50]$	$t \in [1, 10]$	$t \in [11, 20]$	$t \in [21, 30]$	$t \in [31, 40]$	$t \in [41, 50]$
1	1.000	1.000	1.000	1.000	0.922	0.808	0.837	0.843	1.000	1.000
2	0.298	1.000	0.290	1.000	0.171	0.726	1.000	1.000	1.000	0.928
3	1.000	1.000	1.000	1.000	0.179	1.000	1.000	1.000	1.000	1.000
4	1.000	1.000	1.000	1.000	1.000	1.000	0.192	0.198	0.149	1.000
5	1.000	0.648	0.599	1.000	0.286	0.448	0.611	0.612	0.612	0.525
6	1.000	0.212	0.144	1.000	0.003	1.000	1.000	1.000	1.000	0.007
7	1.000	1.000	1.000	0.277	0.043	0.767	0.552	0.866	0.253	1.000
8	1.000	1.000	1.000	1.000	0.895	1.000	0.422	0.422	1.000	0.623
9	0.374	0.446	0.336	1.000	0.180	1.000	1.000	1.000	1.000	0.952
10	1.000	1.000	0.815	0.138	0.021	0.851	0.714	0.634	0.130	0.021
11	1.000	1.000	0.689	0.124	0.020	1.000	0.766	0.730	0.187	0.032
12	0.883	0.974	0.868	0.423	0.130	0.886	1.000	1.000	1.000	1.000

Table 14 continued

h	Tomography					Ventilator				
	$t \in [1, 10]$	$t \in [11, 20]$	$t \in [21, 30]$	$t \in [31, 40]$	$t \in [41, 50]$	$t \in [1, 10]$	$t \in [11, 20]$	$t \in [21, 30]$	$t \in [31, 40]$	$t \in [41, 50]$
13	0.844	0.974	1.000	0.815	0.566	1.000	1.000	1.000	1.000	1.000
14	1.000	1.000	0.290	0.283	0.227	0.624	1.000	0.918	0.918	0.883
15	0.290	1.000	1.000	0.222	0.142	0.782	0.842	1.000	1.000	1.000
16	1.000	1.000	1.000	0.344	0.190	1.000	1.000	1.000	0.984	1.000
17	1.000	0.611	1.000	0.488	0.351	0.980	1.000	1.000	1.000	0.993
18	1.000	1.000	0.431	0.435	1.000	0.625	0.625	0.591	0.620	0.256
19	0.249	0.239	1.000	1.000	0.085	1.000	0.355	1.000	0.200	0.103
20	0.774	0.774	0.774	0.243	0.038	0.778	0.778	0.778	0.286	1.000
21	0.000	0.000	0.000	0.000	0.000	1.000	0.000	1.000	0.000	1.000
23	0.515	0.669	0.505	0.526	0.456	0.696	1.000	1.000	1.000	1.000
24	0.180	0.201	1.000	0.031	0.005	0.068	0.111	0.111	1.000	0.006
25	1.000	1.000	1.000	1.000	1.000	0.353	0.365	0.366	1.000	1.000
26	1.000	1.000	0.238	0.238	0.199	0.999	1.000	1.000	1.000	1.000
27	1.000	1.000	0.716	0.120	0.019	0.199	0.267	0.209	0.041	1.000
28	1.000	0.166	1.000	1.000	0.003	1.000	0.273	1.000	0.028	1.000
29	1.000	1.000	0.688	1.000	0.016	0.109	1.000	1.000	1.000	1.000
32	1.000	1.000	0.881	0.184	0.029	0.954	1.000	1.000	0.323	0.054
33	0.088	0.097	0.073	0.036	0.031	0.618	1.000	1.000	0.719	1.000
34	0.000	0.000	0.000	0.000	0.000	0.000	1.000	0.000	1.000	0.000
35	0.000	0.000	0.000	0.000	0.000	0.000	0.000	0.000	0.000	0.000
36	0.304	1.000	0.275	1.000	0.008	1.000	1.000	1.000	0.291	0.050

References

Ahmadi-Javid, A., Seyedi, P., & Syam, S. S. (2017). A survey of healthcare facility location. *Computers & Operations Research, 79,* 223–263.

Anparasan, A., & Lejeune, M. (2019). Resource deployment and donation allocation for epidemic outbreaks. *Annals of Operations Research, 283*(1), 9–32.

Bai, L., & Zhang, J. (2014). An incentive-based method for hospital capacity management in a pandemic: The assignment approach. *International Journal of Mathematics in Operational Research, 6*(4), 452–473.

Brandeau, M. L. (2005). Allocating resources to control infectious diseases. In *Operations research and health care* (pp 443–464). Springer.

Buyuktahtakin, I. E., des Bordes, E., & Kıbış, E. Y. (2018). A new epidemics-logistics model: Insights into controlling the Ebola virus disease in West Africa. *European Journal of Operational Research, 265*(3), 1046–1063.

Çakir, E., Taş, M. A., & Ulukan, Z. (2021). Cylindrical neutrosophic fuzzy heuristic approach to locate mobile pandemic test labs. In *2021 IEEE international conference on fuzzy systems (FUZZ-IEEE)* (pp 1–6). IEEE.

Carr, S., & Roberts, S. (2010) Planning for infectious disease outbreaks: A geographic disease spread, clinic location, and resource allocation simulation. In *2010 Winter simulation conference (WSC)*. Citeseer: IEEE.

Cronjé, B. J. (2019). *A framework to support the decision-making process for modelling of communicable diseases*. Ph.D. thesis, Stellenbosch University, Stellenbosch.

Devi, Y., Patra, S., & Singh, S. P. (2021). A location-allocation model for influenza pandemic outbreaks: A case study in India. *Operations Management Research* 1–16.

Du, M., Sai, A., & Kong, N. (2020). A data-driven optimization approach for multi-period resource allocation in cholera outbreak control. *European Journal of Operational Research, 291,* 1106–1116.

Erişkin, L. (2021). Preference modelling in sorting problems: Multiple criteria decision aid and statistical learning perspectives. *Journal of Multi-Criteria Decision Analysis, 28*(5–6), 203–219.

GAMS. (2012). *Release 24.0.1*. Washington, DC: GAMS Development Corporation.

Hashemkhani Zolfani, S., Yazdani, M., Ebadi Torkayesh, A., & Derakhti, A. (2020). Application of a gray-based decision support framework for location selection of a temporary hospital during Covid-19 pandemic. *Symmetry, 12*(6), 886.

Ivanov, D. (2020). Predicting the impacts of epidemic outbreaks on global supply chains: A simulation-based analysis on the coronavirus outbreak (Covid-19/SARS-CoV-2) case. *Transportation Research Part E: Logistics and Transportation Review, 136,* 101922.

Ji, Y., Ma, Z., Peppelenbosch, M. P., & Pan, Q. (2020). Potential association between Covid-19 mortality and health-care resource availability. *The Lancet Global Health, 8*(4), e480.

Kang, C. W., Imran, M., Omair, M., Ahmed, W., Ullah, M., & Sarkar, B. (2019). Stochastic-petri net modeling and optimization for outdoor patients in building sustainable healthcare system considering staff absenteeism. *Mathematics, 7*(6), 499.

Khichar, S., Midha, N., Bohra, G. K., Kumar, D., Gopalakrishanan, M., Kumar, B., et al. (2020). Healthcare resource management and pandemic preparedness for Covid-19: a single centre experience from Jodhpur, India. *International Journal of Health Policy and Management, 9*(11), 493–495.

Lee, C., Thampi, S., Lewin, B., Lim, T., Rippin, B., Wong, W., & Agrawal, R. (2020). Battling Covid-19: Critical care and peri-operative healthcare resource management strategies in a tertiary academic medical centre in Singapore. Anaesthesia.

Lipsitch, M., Finelli, L., Heffernan, R. T., & Leung, G. M., Redd; for the 2009 H1N1 Surveillance Group SC. (2011). Improving the evidence base for decision making during a pandemic: the example of 2009 influenza a/h1n1. *Biosecurity and Bioterrorism: Biodefense Strategy, Practice, and Science, 9*(2), 89–115.

Long, E. F., Nohdurft, E., & Spinler, S. (2018). Spatial resource allocation for emerging epidemics: A comparison of greedy, myopic, and dynamic policies. *Manufacturing & Service Operations Management, 20*(2), 181–198.

Luo, H., Liu, J., Li, C., Chen, K., & Zhang, M. (2020). Ultra-rapid delivery of specialty field hospitals to combat Covid-19: Lessons learned from the Leishenshan hospital project in Wuhan. *Automation in Construction, 119,* 103345.

Maleki Rastaghi, M., Barzinpour, F., & Pishvaee, M. S. (2018). A multi-objective hierarchical location-allocation model for the healthcare network design considering a referral system. *International Journal of Engineering, 31*(2), 365–373.

Moghadas, S. M., Shoukat, A., Fitzpatrick, M. C., Wells, C. R., Sah, P., Pandey, A., et al. (2020). Projecting hospital utilization during the Covid-19 outbreaks in the United States. *Proceedings of the National Academy of Sciences, 117*(16), 9122–9126.

Mwandri, M., Hardcastle, T. C., Sawe, H., Sakita, F., Mfinanga, J., Urassa, S., et al. (2020). Trauma burden, patient demographics and care-process in major hospitals in Tanzania: A needs assessment for improving healthcare resource management. *African Journal of Emergency Medicine, 10,* 111–117.

Narula, S. C., & Ogbu, U. I. (1979). An hierarchal location-allocation problem. *Omega, 7*(2), 137–143.

Nikolopoulos, K., Punia, S., Schäfers, A., Tsinopoulos, C., & Vasilakis, C. (2020). Forecasting and planning during a pandemic: Covid-19 growth rates, supply chain disruptions, and governmental decisions. *European Journal of Operational Research, 290*(1), 99–115.

Noronha, K. V. M. S., Guedes, G. R., Turra, C. M., Andrade, M. V., Botega, L., Nogueira, D., et al. (2020). The Covid-19 pandemic in brazil: analysis of supply and demand of hospital and ICU beds and mechanical ventilators under different scenarios. *Cadernos de Saúde Pública, 36,* e00115320.

OECD. (2020). *Revenue Statistics in Asian and Pacific Economies 2020*. https://doi.org/10.1787/d47d0ae3-en, https://www.oecd-ilibrary.org/content/publication/d47d0ae3-en.

Ordu, M., Demir, E., Tofallis, C., & Gunal, M. M. (2021). A novel healthcare resource allocation decision support tool: A forecasting-simulation-optimization approach. *Journal of the operational research society, 72*(3), 485–500.

Oueida, S., Kotb, Y., Aloqaily, M., Jararweh, Y., & Baker, T. (2018). An edge computing based smart healthcare framework for resource management. *Sensors, 18*(12), 4307.

Paul, J. A., & Wang, X. J. (2019). Robust location-allocation network design for earthquake preparedness. *Transportation Research Part B: Methodological, 119,* 139–155.

Pouraliakbarimamaghani, M., Mohammadi, M., & Mirzazadeh, A. (2018). A multi-objective location-allocation model in mass casualty events response. *Journal of Modelling in Management*.

R Core Team. (2017). *R: A language and environment for statistical computing*. Vienna: R Foundation for Statistical Computing.

Revelle, C., Marks, D., & Liebman, J. C. (1970). An analysis of private and public sector location models. *Management Science, 16*(11), 692–707.

Sarkar, J., & Chakrabarti, P. (2020). A machine learning model reveals older age and delayed hospitalization as predictors of mortality in patients with Covid-19. medRxiv.

Savachkin, A., & Uribe, A. (2012). Dynamic redistribution of mitigation resources during influenza pandemics. *Socio-Economic Planning Sciences, 46*(1), 33–45.

Sharma, A., & Mansotra, V. (2014). Emerging applications of data mining for healthcare management-a critical review. In *2014 International conference on computing for sustainable global development (INDIACom)* (pp. 377–382). IEEE.

Pouraliakbarimamaghani, M., Mohammadi, M., & Mirzazadeh, A. (2018). A multi-objective location-allocation model in mass casualty events response. *Journal of Modelling in Management, 13*(1), 236–274.

Snyder, L. V., & Daskin, M. S. (2006). Stochastic p-robust location problems. *IIE Transactions, 38*(11), 971–985.

Sun, L., DePuy, G. W., & Evans, G. W. (2014). Multi-objective optimization models for patient allocation during a pandemic influenza outbreak. *Computers & Operations Research, 51,* 350–359.

Toner, E., & Waldhorn, R. (2006). What hospitals should do to prepare for an influenza pandemic. *Biosecurity and Bioterrorism: Biodefense Strategy, Practice, and Science, 4*(4), 397–402.

Verhagen, M. D., Brazel, D. M., Dowd, J. B., Kashnitsky, I., & Mills, M. (2020). *Predicting peak hospital demand: Demographics, spatial variation, and the risk of "hospital deserts" during COVID-19 in England and Wales*. Oxford

WHO. (2020). *WHO timeline-Covid-19*. WHO (World Health Organization). Retrieved 21 October, 2020 from https://www.who.int/news-room/detail/27-04-2020-who-timeline---covid-19.

WHO, et al. (2021). *Coronavirus disease (COVID-19): situation report*. WHO (World Health Organization).

Woodul, R. L., Delamater, P. L., & Emch, M. (2019). Hospital surge capacity for an influenza pandemic in the triangle region of North Carolina. *Spatial and Spatio-Temporal Epidemiology, 30,* 100285.

Wu, Z., & McGoogan, J. M. (2020). Characteristics of and important lessons from the coronavirus disease 2019 (Covid-19) outbreak in China: Summary of a report of 72 314 cases from the Chinese center for disease control and prevention. *JAMA, 323*(13), 1239–1242.

Xie, J., Tong, Z., Guan, X., Du, B., Qiu, H., & Slutsky, A. S. (2020). Critical care crisis and some recommendations during the COVID-19 epidemic in China. *Intensive care medicine, 46*(5), 837–840.

Yang, J., & Cheng, Q. (2020). The impact of organisational resilience on construction project success: Evidence from large-scale construction in China. *Journal of Civil Engineering and Management, 26*(8), 775–788.

Yang, X., Yu, Y., Xu, J., Shu, H., Liu, H., Wu, Y., & Shang, Y. (2020). Clinical course and outcomes of critically ill patients with SARS-CoV-2 pneumonia in Wuhan, China: a single-centered, retrospective, observational study. *The Lancet Respiratory Medicine, 8*(5), 475–481.

Zheng, Y. J., Yu, S. L., Yang, J. C., Gan, T. E., Song, Q., Yang, J., & Karatas, M. (2020). Intelligent optimization of diversified community prevention of Covid-19 using traditional Chinese medicine. *IEEE Computational Intelligence Magazine, 15*(4), 62–73.

Zinouri, N. (2016). *Improving healthcare resource management through demand prediction and staff scheduling*. Ph.D. thesis, Clemson University.